Carbonaceous species and humic like substances (HULIS) in Arctic snowpack during OASIS field campaign in Barrow

Didier Voisin, Jean-Luc Jaffrezo, Stéphan Houdier, Manuel Barret, Julie Cozic, Martin D. King, James L. France, Holly J. Reay, Amanda Grannas, Gregor Kos, et al.

Carbonaceous species and humic like substances (HULIS) in Arctic snowpack during OASIS field campaign in Barrow

Didier Voisin,[1] Jean-Luc Jaffrezo,[1] Stéphan Houdier,[1] Manuel Barret,[1] Julie Cozic,[1] Martin D. King,[2] James L. France,[2] Holly J. Reay,[2] Amanda Grannas,[3] Gregor Kos,[4] Parisa A. Ariya,[4] Harry J. Beine,[5] and Florent Domine[1,6]

Received 28 July 2011; revised 18 March 2012; accepted 19 March 2012; published 5 May 2012.

[1] Snowpacks contain many carbonaceous species that can potentially impact on snow albedo and arctic atmospheric chemistry. During the OASIS field campaign, in March and April 2009, Elemental Carbon (EC), Water insoluble Organic Carbon (WinOC) and Dissolved Organic Carbon (DOC) were investigated in various types of snow: precipitating snows, remobilized snows, wind slabs and depth hoars. EC was found to represent less than 5% of the Total Carbon Content (TCC = EC + WinOC + DOC), whereas WinOC was found to represent an unusual 28 to 42% of TCC. Snow type was used to infer physical processes influencing the evolution of different fractions of DOC. DOC is highest in soil influenced indurated depth hoar layers due to specific wind related formation mechanisms in the early season. Apart from this specific snow type, DOC is found to decrease from precipitating snow to remobilized snow to regular depth hoar. This decrease is interpreted as due to cleaving photochemistry and physical equilibration of the most volatile fraction of DOC. Depending on the relative proportions of diamond dust and fresh snow in the deposition of the seasonal snowpack, we estimate that 31 to 76% of DOC deposited to the snowpack is reemitted back to the boundary layer. Under the assumption that this reemission is purely photochemical, we estimate an average flux of VOC out of the snowpack of 20 to 170 $\mu g_C\ m^{-2}\ h^{-1}$. Humic like substances (HULIS), short chain diacids and aldehydes are quantified, and showed to represent altogether a modest (<20%) proportion of DOC, and less than 10% of DOC + WinOC. HULIS optical properties are measured and could be consistent with aged biomass burning or a possible marine source.

Citation: Voisin, D., et al. (2012), Carbonaceous species and humic like substances (HULIS) in Arctic snowpack during OASIS field campaign in Barrow, *J. Geophys. Res.*, *117*, D00R19, doi:10.1029/2011JD016612.

1. Introduction

[2] Snowpacks contain many carbonaceous species. Some are present as insoluble grains (e.g., Black Carbon, BC), others are adsorbed at the surface of the ice crystals (e.g., phenanthrene [*Domine et al.*, 2007]), or dissolved in the ice volume (e.g., formaldehyde, [*Barret et al.*, 2011a]). This carbonaceous material affects the role of snow in climate change [e.g., *Flanner et al.*, 2009] and arctic atmospheric chemistry [e.g., *Brock et al.*, 2011], and has therefore been the object of many recent investigations.

[3] Snow albedo is a strong function of the amount of light-absorbing impurities in the snow [*Warren and Wiscombe*, 1980], and so is the surface energy budget of polar regions. In particular, Black Carbon is estimated to have a significant effect on the snow cover life cycle [*Flanner et al.*, 2009; *Yasunari et al.*, 2011]. The presence of carbonaceous absorbing impurities in the snow will also change UV light penetration and influence photochemical reaction rates in the snowpack [*King and Simpson*, 2001; *Grannas et al.*, 2007]. This can be important as snow photochemistry has a deep impact on the overlying atmospheric boundary layer chemical composition. Snow is a source of NO_x [*Honrath et al.*, 1999, 2000] from nitrate photolysis. Snow is also a source of formaldehyde [*Perrier et al.*, 2002], nitrous acid (HONO) or hydrogen peroxide (H_2O_2), which can all photolyze in the dim light of the early polar sunrise and provide OH radicals [*Domine and Shepson*, 2002]. Although the exact mechanism of HONO production from nitrate photolysis is still

[1]Université Joseph Fourier – Grenoble 1/CNRS – INSU, Laboratoire de Glaciologie et Géophysique de l'Environnement, Saint-Martin-d'Hères, France.
[2]Department of Earth Sciences, Royal Holloway University of London, Egham, UK.
[3]Department of Chemistry, Villanova University, Villanova, Pennsylvania, USA.
[4]Department of Chemistry, McGill University, Montreal, Quebec, Canada.
[5]LAWR, University of California, Davis, California, USA.
[6]Takuvik Joint International Laboratory, Université Laval (Canada) and CNRS (France), Quebec, Quebec, Canada.

Corresponding Author: D. Voisin, Université Joseph Fourier – Grenoble 1/CNRS – INSU, Laboratoire de Glaciologie et Géophysique de l'Environnement, 54 rue Molière, F-38402 Saint-Martin-d'Hères, France. (didier.voisin@ujf-grenoble.fr)

0148-0227/12/2011JD016612

unclear, it depends on snow acidity and possibly on the presence of organic photosensitizers, such as humic like substances (HULIS) [*Beine et al.*, 2006, 2008; *Bartels-Rausch et al.*, 2010]. HULIS are a mixture of high molecular weight, highly oxidized, structurally complex organic molecules, somewhat similar to humic and fulvic acids found in surface waters [*Graber and Rudich*, 2006]. They represent an important fraction of marine, soil dust, biomass-burning, biogenic and urban fine organic aerosol, and present a soluble and an insoluble fraction [*Havers et al.*, 1998; *Decesari et al.*, 2001; *Mayol-Bracero et al.*, 2002; *Cavalli et al.*, 2004; *Feczko et al.*, 2007; *Baduel et al.*, 2010]. These complex organics are also effective UV-Vis absorbers. They could explain part of the absorbance of melted snow, as measured by *Anastasio and Robles* [2007] in Greenland that could not be attributed to the measured nitrate and hydrogen peroxide. Together with other high molecular weight carbonaceous species, HULIS are also the most likely photochemical precursors of the observed Volatile Organic Compounds (VOCs) fluxes coming out of the snow [*Boudries et al.*, 2002]. Finally, carbonaceous compounds in the snow also encompass a variety of semi volatile organic compounds (SVOCs), including persistent organic pollutants (POPs), which are known to be deposited in the Arctic from long range transport (see special issue "AMAP Assessment 2009 - Persistent Organic Pollutants (POPs) in the Arctic" in *Science of the Total Environment*, *408*, pp. 2851–3051, 2010), or even photochemically produced in the snow [*Klánová et al.*, 2003; *Grannas et al.*, 2007; *Matykiewiczová et al.*, 2007].

[4] Studies of carbonaceous species in snow usually focus on one of the specific aspects mentioned above. Thus only part of the carbonaceous content of the snow is measured in such studies. The recent overviews on absorbing species in snow by *Hegg et al.* [2010] and *Doherty et al.* [2010] are a good example of a wide spatial coverage of only one specific parameter (namely Black Carbon concentration). An example of a very detailed analysis of the life cycle of some carbonaceous species in snow is that of carbonyl species during the ALERT2000 field campaign [*Boudries et al.*, 2002; *Guimbaud et al.*, 2002; *Houdier et al.*, 2002; *Perrier et al.*, 2002]. A number of comprehensive POPs reviews are available for Arctic regions, some of which have focused specifically on POPs in snowpack [*Garbarino et al.*, 2002; *Melnikov et al.*, 2003; *Usenko et al.*, 2005; *Lafrenière et al.*, 2006]. Several recent lab and modeling studies also point to the importance of snowpack on the ultimate fate of POPs in snow covered regions [*Meyer et al.*, 2009a, 2009b; *Meyer and Wania*, 2011]. Probably the only example of a comprehensive description of carbonaceous compounds in snow/ice is the study by *Legrand et al.* [2007a] which focused on interpreting carbonaceous content in an Alpine ice core in terms of atmospheric organic aerosol signal.

[5] Such a comprehensive representation of carbonaceous species in Arctic snow is the focus of the present work, which was performed during the OASIS field campaign in Barrow. This study had several objectives: (1) build a data set for use in future snow photochemistry modeling studies in conjunction with the data on meteorology and gas phase composition available from the campaign; (2) provide data on organic absorbers for comparison with optical measurement in the snow [*Beine et al.*, 2011; *France et al.*, 2012]; (3) use this data set for a better understanding of physical and chemical processes influencing snow chemical composition. In this perspective, special attention is placed on major classes of carbonaceous species, defined operationally: Elemental Carbon (EC, closely linked to BC, but measured by thermo optical transmission method instead of a purely optical method); Water Insoluble Organic Carbon (WInOC); Dissolved Organic Carbon (DOC), which altogether represent the Total Carbon Content (TCC = EC + WInOC + DOC) of the snowpack. Among DOC species, we will focus on soluble HUmic LIke Substances (HULIS), C2–C5 dicarboxylic acids and short chain aldehydes, as these compounds are involved in snow photochemistry, especially soluble HULIS, whose optical properties (UV-Vis absorbance) are measured and discussed.

2. Using Snow Physics to Understand Snow Chemistry, and Vice Versa

2.1. Snow Physics and Its Impact on Chemistry

[6] Snow formation and physical evolution (metamorphism) are known to affect snow chemical reactivity and composition [*Domine et al.*, 2008]. These possible interactions are illustrated in Figure 1. Once on the ground, five different processes primarily modify the carbon content of the snow:

[7] 1. *Physical equilibration with the surrounding atmosphere*: is relevant only for volatile species. It depends on the concentration in the snow relative to the atmosphere and on temperature through the thermodynamics of the specific partition process. Physical processes involved may be adsorption/desorption (e.g., for phenanthrene [*Domine et al.*, 2007]), solid state diffusion (e.g., for formaldehyde [*Barret et al.*, 2011b]) or liberation/trapping by sublimation/condensation processes during metamorphism. The kinetics of this equilibration is certainly enhanced by snowpack ventilation (wind pumping), active metamorphism, such as during depth hoar formation [*Marbouty*, 1980], or when snow grains become air borne and sublimate (e.g., *Barret et al.* [2011b] for formaldehyde).

[8] 2. *Photochemical fragmentation*: OH is formed in the snowpack, mainly from NO_3^-, H_2O_2 and NO_2^- photolysis [*Anastasio et al.*, 2007]. These radicals can induce oxidative cleaving of longer chain carbonaceous species and produce VOCs. Depending on their partitioning between air and ice, these VOCs eventually get released to the interstitial air and the atmosphere, which causes carbon loss for the snowpack.

[9] 3. *Photochemical functionalization*: photochemistry in the snowpack does not always cleave carbonaceous species to produce VOCs. Photochemistry can also oxidize the existing carbonaceous species without breaking C-C bonds, making these species more water soluble, and less volatile. Obviously, functionalization and fragmentation are both oxidative processes and their separation is somewhat artificial, but useful as it implies a different fate for the impacted carbon load.

[10] 4. *Dry deposition through wind pumping*: snow can trap aerosol particles when air circulates through it. This increases the carbon load of surface snow through deposition of WinOC and DOC from the aerosol, impacting the less volatile fraction of DOC. The effectiveness of this process has been investigated in a very detailed manner for sea salt [*Domine et al.*, 2004]. We can assume that this process also

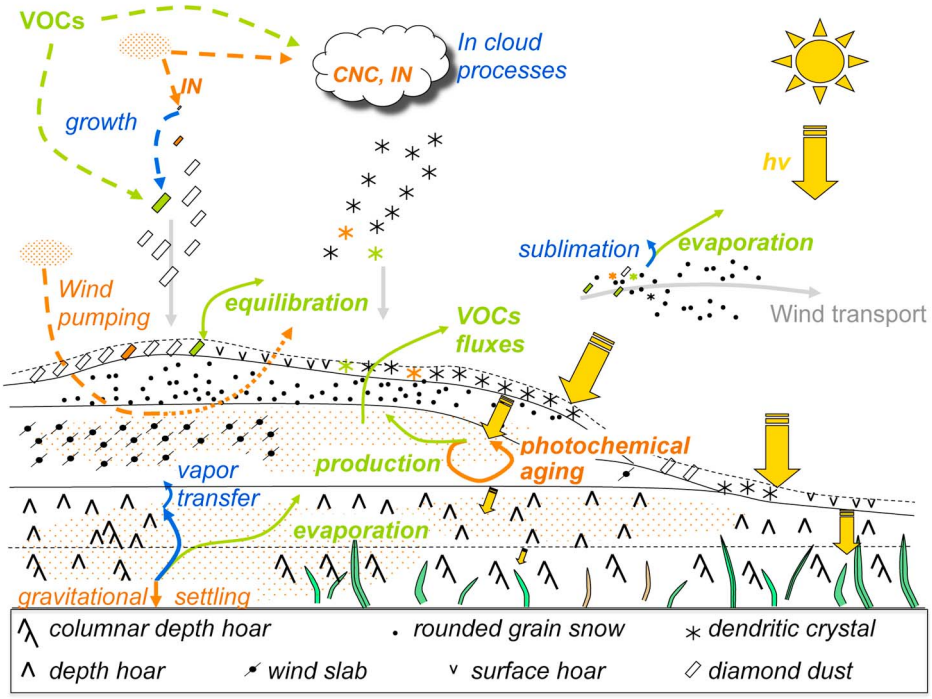

Figure 1. Illustration of the main physical and chemical processes that are expected to be involved in explaining the observed different chemical composition of various snow types. Arrows describing the photon flux decrease with depth to illustrate absorption of radiations by the snowpack. The illustrated stratigraphy is a simplified version of the typical Barrow snowpack, and includes the existence of outcropping layers of old depth hoar; it has a typical vertical extent of ~50 cm.

exists for the carbonaceous fraction, with an importance possibly depending on aerosol size.

[11] 5. *Gravitational deposition at the base of depth hoar layers*: during depth hoar formation, intense water vapor transfer occurs, and 60% of the ice lattice can go through at least one evaporation – condensation cycle in 12 h [*Pinzer and Schneebeli*, 2009]. Aerosol particles deposited at the surface of snow grains could in such circumstances fall toward the bottom of the depth hoar layer. Such a "self-cleaning" process was suggested by *Doherty et al.* [2010] to explain an observed BC depletion in depth hoar layers in Siberia. This process, if it exists, would only impact the most non-volatile and hydrophobic species of the carbon pool.

[12] Chemical composition can be used to probe these mechanisms, if we can trace the physics that potentially affected our snow samples. This physics governing the morphology of snow results from the metamorphic history of the snow layer, and thus keeps a track of the physics responsible for its evolution.

2.2. Carbon Speciation as Influenced by Snow Physics

[13] In our carbon speciation, the various fractions are influenced differently by number of processes. Organic carbon in the snow is either water insoluble (WinOC) or water soluble (DOC). WinOC corresponds to the water insoluble organic carbon present in aerosol or soil particles, or vegetal debris deposited to the snow. It will for example contain long chain (C18 to C22) fatty acids coming from decomposing cells of various origins, or long chain alkanes (hopanes and steranes) from incomplete combustions. Photochemistry can decrease WinOC in the surface snowpack by: (1) photochemical fragmentation followed by VOCs reemission to the atmosphere or (2) transformation into DOC by photochemical functionalization. Some specific processes of this latter kind have been largely described in the aerosol, such as the production of diacids from fatty acids [*Chebbi and Carlier*, 1996; *Kawamura et al.*, 1996], and could very well occur in aerosol particles at the surface of snow grains.

[14] DOC is made up of more or less volatile species. The first category typically covers atmospheric VOCs, and is represented in our speciation by aldehydes such as formaldehyde, glyoxal and methylglyoxal. Thermodynamic data for the interactions of those species with ice are only available for formaldehyde [*Barret et al.*, 2011a]. This first category also covers VOCs such as acetophenone and monoacids, incorporated to the snow either during its formation or later on the ground. The second category typically covers the water soluble fraction of the organic content of atmospheric aerosol, as well as species produced by functionalization of carbonaceous species in the snow. These are represented in our speciation by diacids (oxalic, succinic and glutaric acids) and the operationally defined polyacidic soluble HULIS.

[15] This understanding of the possible fate of our carbon pools can be used either to trace processes with species whose physics is known (e.g., formaldehyde [*Barret et al.*, 2011b]), or to give indications on species fate according to their reaction to certain processes.

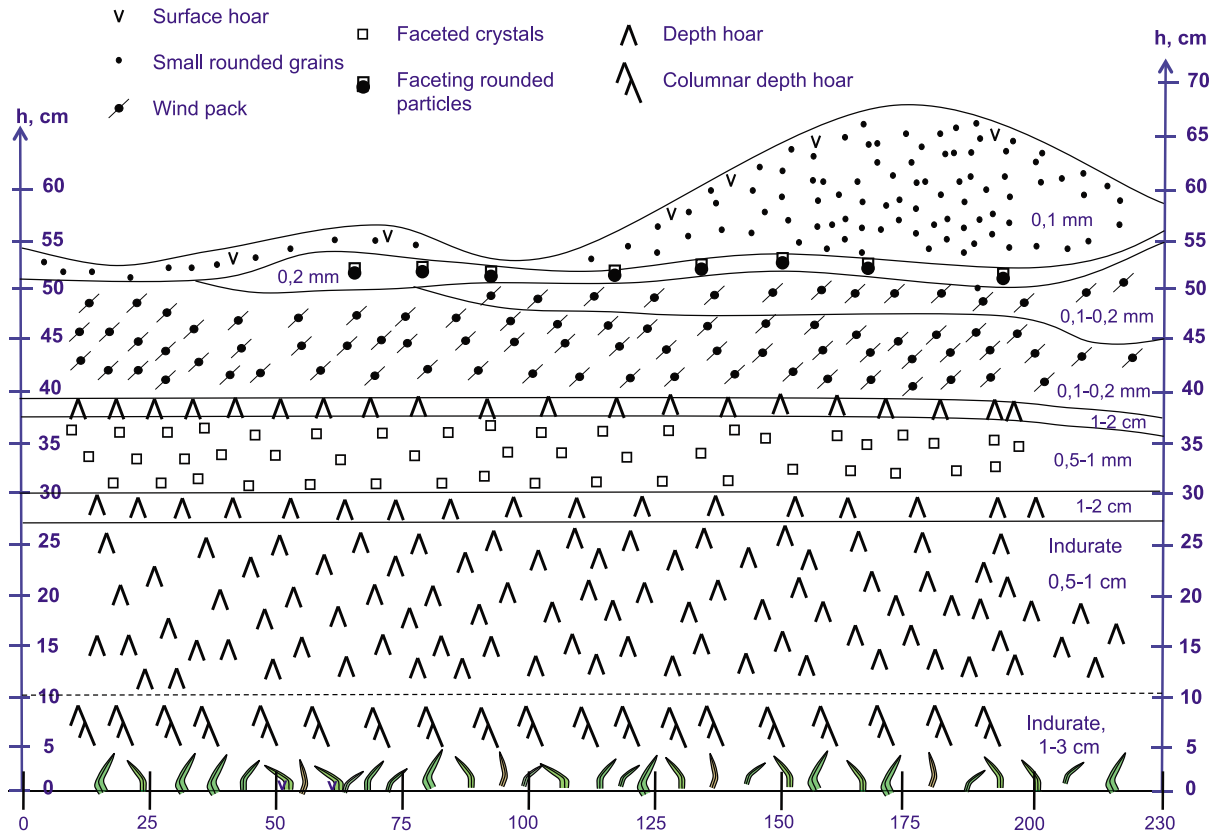

Figure 2. Typical visual stratigraphy for Barrow snowpacks. Layers of small rounded grains are soft layers typically produced by the recent deposition of wind-drifted snow. Wind slabs represent the same kind of deposit, only older and sintered over time. Faceted crystals and depth hoar result from temperature gradient metamorphism that produces water vapor remobilization through the snowpack. Faceted crystal can indicate either early stages of depth hoar formation, or lower values of the temperature gradients, so that the depth hoar stage is never reached. Note that heavily metamorphosed layers are visually homogeneous at a few meters horizontal scale, whereas younger, less transformed layers are clearly discontinuous at this length scale.

2.3. Snow Sampling

[16] Sampling for TCC took place during the OASIS field campaign in Barrow, Alaska, from February 20th to April 20th, 2009, and was led in coordination with a survey of the total absorption of melted filtered snow [*Beine et al.*, 2011]. Part of the sampling was coordinated with Persistent Organic Pollutants sampling in the snow and air, as well as with a survey of Semi Volatile Organic Compounds and biological material in the snow. Most of the samples were collected at the main snow sampling area, about 300 m from the BARC building, around the point (71°19.395′N, 156°39.685′W), except for a specific subset collected 9 miles inland.

[17] The snowpack stratigraphy at Barrow is determined by wind and metamorphism, rather than by precipitation [*Domine et al.*, 2012]. Precipitation events are not frequent, while wind storms are. Wind storms raise snow, which then accumulates in discontinuous patches. All snow layers are therefore discontinuous (see Figure 2). As it partly reflects the history of the sampled snow, each sample was classified according to 8 subtypes that can be grouped into 4 main categories.

[18] The first category represents freshly precipitated snow, and includes Fresh Snow and a mixed Diamond Dust – Surface Hoar subtype. Diamond dust formation, and its physical and chemical characteristics are discussed in detail by *Domine et al.* [2011]. Diamond dust (DD) is clear sky precipitation, and usually forms under strong temperature inversion and low wind conditions, which are also conditions under which surface hoar forms, so that both were often sampled together. Visually, 10–40% of the collected mass was surface hoar (SH). Fresh Snow is here precipitating snow formed in clouds, usually at higher altitude, and potentially involving some mixed phase processes such as riming. In low wind conditions, such newly precipitated snow could form a thin (<1 cm) homogeneous continuous layer at the surface of the snowpack. It was the case for DD – SH, and has been the case for one of the two fresh snow events observed (April 5th).

Figure 3. Photograph of a common feature of the Arctic snowpack: a thin layer of old snow, heavily metamorphosed into depth hoar, lets grass stick out. This picture was taken on 7 March 2009 ~ 100 m from the BARC building in Barrow.

[19] The second category represents wind remobilized snow and includes drifting snow and recent snow drifts. Drifting snow was collected during wind events, by digging a small hole in the snowpack, letting a vial sit there for a few minutes, where it would spontaneously fill up. In some cases, such as on March 9th, there was recognizable fresh snow crystals mixed with remobilized snow. As there is no chemical difference between this particular event and other drifting snow events, the two samples from this event were labeled as drifting snow. Recent snow drifts, which are recent wind-deposited snow, were easily identified on the ground as loosely packed snow, usually downwind of small ridges in the snowpack surface, and not yet sintered.

[20] The third category represents wind slabs, as commonly observed in Barrow, and was split in 2 subtypes: a wind slab is the sintered evolution of the recent snow drift subtype, typically formed during the last wind spell; eroded wind slabs were still older, showing clear marks of wind erosion, suggesting a formation older than the last wind remobilization episode. In the absence of fresh precipitation on the surface and as already described by *Domine et al.* [2002], the surface of the snowpack was for the most part a random assemblage of those last 4 snow subtypes, of varied age and history. Another outcropping snow type was a mm-thick melt-freeze crust, resistant to wind erosion, but which was too thin to be sampled alone. In the absence of recent precipitation, this melt-freeze crust covered over a third of the snow surface.

[21] The last category represents depth hoar layers, formed by snow metamorphism mainly at the beginning of the season, when strong temperature gradients prevail in the shallow snowpack, between the cold air and the ground that is still warm [*Domine et al.*, 2002]. If the initial snow is very dense, then indurated depth hoar forms, which is a mixture of columnar depth hoar and rounded grains remaining from the initial wind slab. Depth hoar formation can erase the boundary between layers created by wind, so that there often appears to be a homogeneous depth hoar layer at the base of the snowpack (see Figure 2). Depending on subsequent snow erosion, this layer can sometime become exposed, as seen in Figure 3, where grass stick out of a thin (~10–15 cm) indurated depth hoar layer. Those depth hoar layers, however, can have very heterogeneous chemical composition.

[22] Except for POPs, where the volume needed per sample was too big (~50 L), care was taken to sample into homogeneous-looking layers of the visually identified stratigraphy. Table 1 gives the number of samples analyzed for each snow type. Some snow types (precipitating snow and depth hoar) are clearly under represented, especially for EC/WinOC, soluble HULIS and POPs. The initial focus of the sampling was on surface exchanges, explaining why depth hoars are under represented; also, precipitating snow only appeared as millimeters thick layers, making it uneasy to sample enough material for EC/WinOC, soluble HULIS and POP analysis.

3. Experimental Methods

3.1. Total Carbon Content Determination

[23] Snow was collected with stainless steel instruments and stored frozen (−30°C) in pre-cleaned borosilicate glass bottles until further processing. Samples for DOC measurements were shipped frozen to Grenoble, where DOC was measured on filtered samples (Acrodisc 0.22 μm) with a Shimadzu TOC-V_{CSH} instrument by catalytic conversion to CO_2 on a Pt wool at high temperature (680°C), followed by NDIR detection. Procedural blanks (N = 50) were obtained by filtering 20 mL of Elgastat™ grade ultrapure water, giving an average value of 25 ± 3 $\mu g_C\ L^{-1}$, which was subtracted from measured DOC concentrations. Each sample was measured 5 times, from 2 mL injections, and the reported uncertainties account for standard deviation on those 5 determinations plus the blank variability. These

Table 1. Number of Samples Analyzed for Each Snow Type

	Diamond Dust	Fresh Snow	Drifting Snow	Blown Snow	Wind Slab	Eroded Wind Slab	Depth Hoar	Indurated Depth Hoar
EC / WinOC	1		9	16	13	9	1	1
DOC	7	4	15	32	26	13	6	6
Dicarboxylics	7	4	15	32	26	13	6	6
HULIS	3				20			
Aldehydes	50	18	18	27	31		11	13
POPs	5					18		5
SVOCs			3	1		3		

uncertainties have a median value of 6% of the reported DOC concentration and exceed 17% for only 5% of our samples.

[24] For the analysis of EC / WinOC, snow was melted within 1 or 2 days following sampling, and filtered on pre-combusted QMA quartz filters. All filters were stored frozen and shipped back to Grenoble. EC / WinOC was quantified on the entire filter (21 mm diameter) by a Thermal Optical Transmission method (Sunset Lab instrument), following the EUSAAR-2 protocol [*Cavalli et al.*, 2010]. Filtration blanks were prepared in the field by filtering 1 L of milliQ water (obtained from the BARC facilities), shipped and analyzed with the samples. This blank was 7 ± 2 μg_C L^{-1} for WinOC and below the detection limit for EC; it was subtracted from the measured values. Filtration efficiency was evaluated by measuring the carbon content on a backup filter placed immediately after the analytical filter. Losses were found to be lower than 5% for both WinOC and EC, which is as good as or better than losses mentioned by previous investigators using similar filtration techniques [*Ducret and Cachier*, 1992; *Lavanchy et al.*, 1999].

3.2. Volatile Organic Compounds

[25] Determination of volatile organic compounds employing solid phase microextraction (SPME) with gas chromatography and mass spectrometric detection (GC-MS) was performed following a previous study [*Kos and Ariya*, 2006]. In brief, pre-cleaned brown glassware was used for storage of surface snow samples (0–3 cm). After transport to the McGill laboratory in Montreal in frozen state, samples were melted and temperature equilibrated immediately before analysis in 20 mL custom-made Pyrex flasks. Flasks were filled to the PTFE-lined silicone septum (Chromatographic Specialties, Brockville, ON, Canada) to minimize headspace losses and stirred using a magnetic stirrer, while the SPME fiber was immersed in the sample for 40 min. A divinylbenzene (DVB)-coated polydimethylsiloxane (PDMS) fiber with a film thickness of 65 μm was employed. Identically treated field and laboratory Milli-Q water blanks were used to check for procedural contamination. After adsorption, the fiber was immediately desorbed into the GC–MS injector of a Hewlett–Packard gas chromatograph with single-quadrupole mass spectrometric detection (GC–MS, HP GC 6890 and MSD 5973, Agilent Technologies, Mississauga, ON, Canada). Mass spectra were analyzed with the NIST MS Search 2.0 program (NIST, Gaithersburg, MD, USA) and HP Chemstation software.

3.3. Organochlorine

[26] Snow for organochlorine analysis was sampled using hexane-rinsed steel shovels and collected in hexane-rinsed Teflon bags, which were housed in 20 L buckets for transport. In most cases, two buckets were filled for each snow sample, giving a combined mass of 15–20 kg. In the laboratory sealed sample buckets were allowed to melt until they reached 25°C. Melted samples were passed through glass columns containing XAD resin precleaned by accelerated solvent extraction (ASE; Dionex 2000, Sunnyvale, California) using a three-step extraction sequence (100% acetone; 75%/25% acetone/hexane; 50%/50% acetone/hexane). The concentration of all analytes in the final cleaning extract was below the instrumental limit of detection for each analyte. After sample extraction the XAD resin was transferred to a glass storage vial, spiked with 10 ng of 2,2′,3,3′4,4′-hexachlorobiphenyl (PCB 128; Ultra Scientific, Kingston, RI, USA) as an internal recovery standard, and sealed for shipping back to Villanova University. Analytes were recovered from XAD by ASE using a 75%/25% hexane/acetone mix; approximately 10 g of the extract was evaporated to a residual mass of approximately 0.1 g. Determination of organochlorine pesticides and PCBs was carried out using a gas chromatograph (GC, Agilent 6890 N, Agilent Technologies, Palo Alto, CA, USA) fitted with a RTX-5 column (30 m length, 0.25 μm film thickness, Restek, Bellafonte, PA, USA) with mass spectrometric detection (Agilent 5973, Agilent Technologies, Foster City, CA, USA). One μL sample injections were made in pulsed splitless mode at an injector temperature of 250°C. The oven was initially held at 120°C for one minute, ramped at 4°C/minute to 250°C, ramped at 100°C/minute to 320°C then held for three minutes (run time: 37.2 min). The mass spectrometer was run with negative chemical ionization using methane as the reagent gas and the detector in selected ion monitoring (SIM) mode. Two runs were performed for each sample; the first using a SIM program specific to pesticides and the second using a SIM program for PCBs. Quantitation of all analytes was performed using an external standard calibration. Analytical curves were calculated from analyses of mixed calibration standards containing pesticides in hexane within the concentration range between 0.1 and 60 μg L^{-1} for pesticides or 1 to 40 μg L^{-1} for each of seven representative PCB congeners. The concentrations were scaled using the recovered internal standard to account for extraction efficiency, a sample blank correction was applied, and the average concentration of each analyte in the original environmental sample calculated.

3.4. Aldehydes and Dicarboxylic Acids

[27] Dicarboxylic acids (oxalic, malonic, succinic, glutaric) were measured on the same samples as DOC, in Grenoble, by ion chromatography on a Dionex DX500 instrument, following the method described by *Ricard et al.* [2002], resulting in detection limits below 1 $\mu g.L^{-1}$ and typical uncertainty of 10%.

[28] Sampling for aldehydes is described in detail by *Barret et al.* [2011b]. Analysis was conducted in Barrow, according to the method described by *Houdier et al.* [2011], and included formaldehyde, glyoxal, methylglyoxal and acetaldehyde. Briefly, samples were acidified with H_2SO_4 before adding dansylacetamidooxyamine as a derivatization agent. The resulting adducts were separated by HPLC on a C18 column, followed by fluorescence detection, resulting in detection limits below 1 $nmol.L^{-1}$ and typical uncertainties better than $\pm 15\%$ at the 95% level of confidence.

3.5. Soluble HULIS Extraction and Quantification

[29] Soluble HULIS samples were extracted in Barrow within 2 days of their sampling. The soluble HULIS extraction procedure used here is a modified version of a protocol initially developed for the aerosol [*Baduel et al.*, 2009]. A total volume of 300 to 900 mL of melted snow was passed by a controllable syringe pump through a DEAE column (GE Healthcare®, HiTrap™ DEAE FF, 0.7 cm ID × 2.5 cm length) at a 1.5 mL min^{-1} flow rate. A precleaned

online filter (Acrodisk®, 0.22 μm porosity) was installed between the syringe pump and the resin for each new sample, and removed before the elution step. After this charging step, the resin is washed with 6 mL of ultrapure water (resistivity >18 MΩ.cm) to remove neutral components and hydrophobic bases. Then, mono- and di-acids together with some anionic inorganic species retained in the resin are eluted with 12 mL of a 0.04 M NaOH solution (J.T. Baker®, pro analysis). Finally, the polycharged compounds (HULIS) are quickly eluted into a storage vial using 2.5 mL of a 1 M (Normapur®) sodium chloride solution. After every extraction, the resin was rinsed twice with the elution solutions (NaOH, and NaCl). Every other second rinsing was stored frozen as an extraction blank to be processed back in Grenoble with the regular extracts. As compared to the original procedure used for aerosol [*Baduel et al.*, 2009], the increased flow rate results in a lower retention (87 ± 3% instead of 93 ± 1% at 1 mL.min^{-1} flow rate) of the polycharged (HULIS) fraction, as measured by the recovery of a 50 ng$_C$ g^{-1} solution of Suwanee River Fulvic Acid (IHSS®). This sub optimal flow rate was chosen to keep the charging time reasonable (up to 10 h for 900 mL samples). The measured recovery was accounted for in the reported concentrations.

[30] The carbon content of soluble HULIS extracts and extraction blanks was quantified on a Shimadzu TOC-V$_{CPH}$ instrument by catalytic combustion of 50 μL injections on Pt coated spheres at 680°C in oxygen followed by non dispersive infrared detection of the evolved CO_2. Five replicate measurement for each extract resulted in a median relative standard deviation of 3%. As the soluble HULIS extracts are heavily loaded in salt, ultrapure water was repeatedly injected in the instrument in between two soluble HULIS extracts measurements. The average carbon concentration in the extraction blanks (1.2 ± 0.5 mg$_C$ L^{-1}) was subtracted from the carbon concentration measured in the actual soluble HULIS extracts. The resulting soluble HULIS carbon concentration was rescaled to the extracted volume to yield the soluble HULIS carbon concentration in the sampled snow. The overall uncertainty in soluble HULIS carbon concentration in the snow comes mostly from the dispersion of the subtracted blank and represented a 19% median value. Absorbance spectra of soluble HULIS extracts were measured in a Liquid Chromatography UV-Vis diode array detector (Dionex DAD-340U), with a 2 nm resolution over the range 200–600 nm, at a 2 Hz frequency. A syringe pump was used to inject alternatively ultrapure water (resistivity >18 MΩ.cm, Elgastat® grade) and 1.5 mL of the soluble HULIS extract, at a 0.5 mL min^{-1} flow rate. When the sample is injected, absorption quickly rises to a plateau where it stabilizes. The stable portion of the plateau, lasting 1.2 min (140 individual spectra) was used to get an averaged absorption spectrum, with an uncertainty calculated as the associated standard deviation. Using the length of the optical cell given by the manufacturer (l = 0.9 cm), we calculated from Beer's Law the molar absorptivities of nitrate solutions of varying concentrations (10^{-4} to 2.10^{-3} mol L^{-1}), and found values that agreed within our experimental uncertainties with published data [*Chu and Anastasio*, 2003] in the 280–360 nm range, thus validating our experimental setup. Absorption spectra of all extraction blanks were averaged and this average subtracted from the raw absorption spectra of soluble HULIS extracts to get the net absorption spectra of soluble HULIS extracts. For some soluble HULIS extracts, the measured absorbance was lower than the average absorbance of the blanks plus the standard deviation. These samples were excluded from further analysis. Knowing the carbon concentration $C_{HULIS,extract}$ in the extract, Beer's Law was used to calculate the base 10 HULIS carbon mass absorptivity (in units of cm^2 mg$_C^{-1}$) according to:

$$\epsilon_{HULIS} = A_{extract}/C_{HULIS,\,extract}\,l \tag{1}$$

where $A_{extract}$ is the measured absorbance, and l is the length of the optical cell. Although it is expressed in the same units as the quantity α/ρ used by *Sun et al.* [2007] and *Moosmüller et al.* [2011], it should be noted that it is smaller by a ln(10) factor. Independently of the soluble HULIS carbon concentration measurement, our data has been used to evaluate the contribution of soluble HULIS to the total absorption of melted snow. The results of this specific analysis are reported by *Beine et al.* [2011].

[31] The dependence on wavelength of the calculated carbon mass absorptivities spectra was then evaluated through their Absorption Angström Coefficient (AAC). AAC is calculated between two wavelengths as the exponent of a power law describing the spectrum:

$$\frac{\epsilon_{HULIS}(\lambda_1)}{\epsilon_{HULIS}(\lambda_2)} = \left(\frac{\lambda_1}{\lambda_2}\right)^{-AAC(\lambda_1,\lambda_2)}. \tag{2}$$

[32] The choice of the wavelength pair used for the calculation is important, as AAC is known to depend on wavelength [*Sun et al.*, 2007]. This led *Moosmüller et al.* [2011] to recently propose a one wavelength definition of AAC, as the local slope of the absorptivity curve in a log: log graph, which is the limit of expression (2) when λ_1 and λ_2 get infinitely close:

$$AAC(\lambda) = -\frac{d\ln(\epsilon_{HULIS})}{d\ln\lambda} = -\frac{\lambda}{\epsilon_{HULIS}}\frac{d\epsilon_{HULIS}}{d\lambda}. \tag{3}$$

[33] Since the AAC is essentially a derivative (see equation (3)), it is very sensitive to small variations in the absorption spectrum, as each tiny shoulder in the spectrum translates into a peak in the AAC. This will especially be true for HULIS at higher wavelength, as λ/ϵ_{HULIS} becomes higher and amplifies any peak in the AAC. We thus calculated the AAC at different wavelengths pairs for comparability with other studies, and the wavelength dependant AAC between 250 and 500 nm. The latter was calculated after smoothing the initial spectrum using either a second order Savitsky – Golay algorithm or a running average.

4. Results

4.1. Total Carbon Content Bulk Speciation

[34] Figure 4 shows EC, WinOC and DOC concentrations, as well as TCC = EC + WinOC + DOC, for each snow type. Fresh precipitation and depth hoar are clearly underrepresented in EC and WinOC measurements (1 sample each),

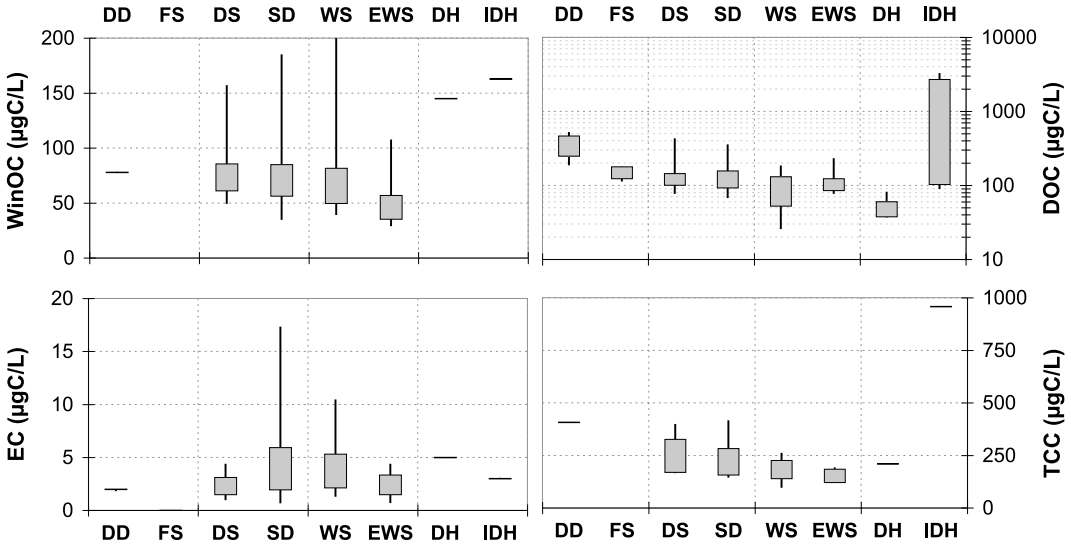

Figure 4. Box and whiskers plots of the concentration of Dissolved Organic Carbon (DOC), Water Insoluble Organic Carbon (WinOC), Elemental Carbon (EC) and Total Carbon Content (TCC = EC + WinOC + DOC) in various snow types (DD: Diamond Dust; FS: Fresh Snow; DS: Drifting Snow; SD: Snow Drifts; WS: Wind Slab; EWS: Eroded Wind Slab; DH: Depth Hoar; IDH Indurated Depth Hoar). The length of each box shows the central 50% of the values (i.e., the bottom and top of each box are the first and third quartile). The lines extend to the Min and Max values. For WinOC and EC (and thus TCC) in depth hoar and diamond dust, there has been only one sample collected, which is shown by the horizontal bar for reference, as it has little statistical significance. Also note that for readability purposes, DOC is on a log scale.

and we will thus discuss TCC only on fine grained snow (wind slabs and remobilized snow). These 4 subtypes of snow samples have rather homogeneous TCC, ranging from 100 to 400 $\mu g_C.L^{-1}$ (median 183 $\mu g_C\ L^{-1}$), which is comparable to the few measurements available from *Grannas et al.* [2004] at Alert in winter (200 and 700 $\mu g_C\ L^{-1}$) and Summit in summer (400 to 500 $\mu g_C.L^{-1}$) and from *Hagler et al.* [2007] at Summit in summer (120 $\pm$ 50 $\mu g_C\ L^{-1}$).

[35] As seen in Figure 4, TCC tends to slightly decrease from Drifting Snow to Eroded Wind slab, i.e., TCC tends to be lower for older snows. As aerosol dry deposition is expected to increase the concentration of any conservative species (such as sea salt, for example) over time after snow precipitation [*Domine et al.*, 2004], the tentatively observed trend implies some loss of carbon from the snowpack over time.

[36] WinOC and DOC together represent the major fraction (over 95%) of carbon in the surface snowpack and remobilized snow. WinOC represent a very significant fraction of TCC in fine grained snows (Figure 5), with some values above 55% (median value 38%; half the values between 28% and 42%), higher than found in Greenland [e.g., *Hagler et al.*, 2007] or more generally in aerosols [e.g., *Jaffrezo et al.*, 2005]. This is not so surprising, as Barrow is a coastal site covered with tundra snowpack, directly in contact with plant and soil material (see Figure 3). It was not uncommon to find plant debris transferred from the $\sim$1 L snow sample to the filter. These were manually removed, but this presence of macroscopic debris strongly suggests some microscopic counterpart as a contribution to WinOC, as already shown by *Grannas et al.* [2004] for Alert samples.

[37] EC only represents up to 5% of TCC, with concentrations in the 2 to 17 $\mu g_C.L^{-1}$ (median 3 $\mu g_C\ L^{-1}$). This is lower than the 8 $\pm$ 3 $\mu g_C\ L^{-1}$ measured at remote locations in the Canadian arctic and around Barrow by *Doherty et al.* [2010], but they used an optical method, calibrated for Black Carbon, which can explain such a discrepancy. Indeed, they measured 2–2.6 $\mu g_C\ L^{-1}$ in surface snow in Summit, when *Hagler et al.* [2007], using the same method we used, measured 0.6 $\pm$ 0.4 $\mu g_C\ L^{-1}$.

[38] DOC concentrations are available in many more samples, therefore allowing a comparison of depth hoar and fresh precipitations with "old" and remobilized fine grained snow. Although DOC concentrations in these surface

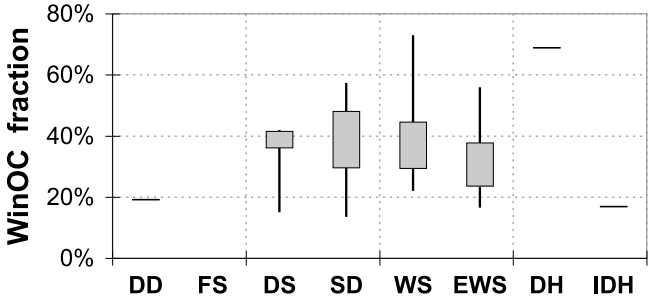

Figure 5. Contribution of Water Insoluble Organic Carbon to the Total Carbon content in various snow types (DD: Diamond Dust; FS: Fresh Snow; DS: Drifting Snow; SD: Snow Drifts; WS: Wind Slab; EWS: Eroded Wind Slab; DH: Depth Hoar; IDH Indurated Depth Hoar).

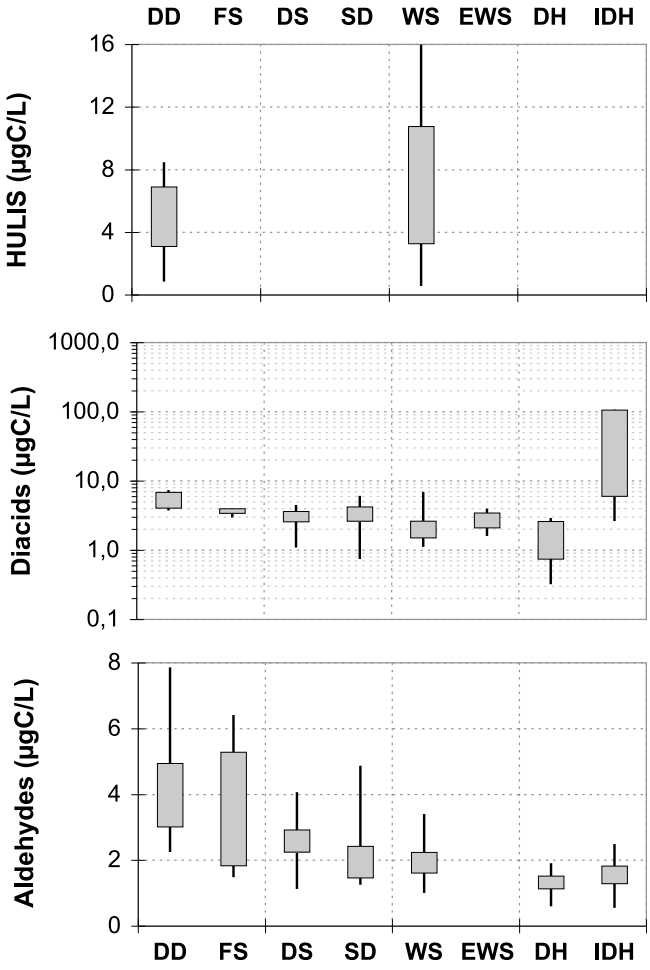

Figure 6. Box and whiskers plots of the concentration in various snow types of organic diacids (oxalic, glutaric, succinic), short chain aldehydes (formaldehyde, acetaldehyde, glyoxal, methylglyoxal) and HULIS, in units of $\mu g_C.L^{-1}$. The length of each box shows the central 50% of the values (i.e., the bottom and top of each box are the first and third quartile). The lines extend to the Min and Max values. Note that for readability, diacids concentrations are on a log scale.

snows are rather homogeneous, with 80% of the values in the 55–174 $\mu g_C\ L^{-1}$ range (median 106 $\mu g_C.L^{-1}$), they tend to decrease in older snow, going from a 330 $\mu g_C\ L^{-1}$ median concentration for Diamond Dust (half the values in the 250–470 $\mu g_C\ L^{-1}$ range) to 135 $\mu g_C\ L^{-1}$ for fresh snow (range 120–180 $\mu g_C\ L^{-1}$), then to 115 $\mu g_C\ L^{-1}$ for freshly remobilized snow (range 90–155 $\mu g_C\ L^{-1}$), to 90 $\mu g_C\ L^{-1}$ for wind slabs (range 60–125 $\mu g_C\ L^{-1}$), down to 55 $\mu g_C\ L^{-1}$ for depth hoar, potentially showing a loss process at work in the snowpack. In stark contrast to this general trend, indurated depth hoar samples show the highest observed DOC concentration, up to 3300 $\mu g_C\ L^{-1}$ (median value 1500 $\mu g_C\ L^{-1}$).

4.2. Dissolved Organic Carbon Speciation

[39] Figure 6 shows the concentrations of diacids (oxalic, succinic, glutaric), aldehydes (formaldehyde, acetaldehyde, glyoxal, methylglyoxal) and HULIS in the investigated snow types. Among the measured aldehydes, as shown in Table 2, formaldehyde is the largest single contributor to the carbon load (on average over half the aldehyde carbon load), followed by glyoxal (on average 1/4 of the aldehyde carbon load). This relative contribution does not change from one snow type to another. Aldehydes concentrations are higher in freshly precipitated snow than in fine grained snow, and their concentration keep increasing with time in the diamond dust layer on the ground until they get remobilized by wind. This is analyzed in detail by *Barret et al.* [2011b] and *Domine et al.* [2011], and interpreted as photochemical production of aldehydes in the snowpack from unknown organic precursors, followed by interstitial air / snow equilibration of the topmost layer. The concentrations of aldehydes tend to decrease in older snows, reaching a minimum in depth hoar layers (Figure 6). Altogether, aldehydes represent 1 to 4% of the DOC load in all snow types, except for wind slabs, where they represent 2 to 10% of the DOC.

Table 2. Contribution of Individual Measured Aldehyde to the Total Aldehyde Carbon Load

	Formaldehyde (%)	Acetaldehyde (%)	Glyoxal (%)	Methylglyoxal (%)
Min	29	1	5	1
First quartile	51	7	17	6
Median	58	11	23	8
Third quartile	64	15	30	12
Max	86	30	63	34

[40] Diacids concentrations and DOC behave similarly in all snow types. Diacids concentrations tend to decrease as snow ages, going from a median value of 5.7 $\mu g_C\ L^{-1}$ in diamond dust (half the values are in the range 4.1–6.9 $\mu g_C\ L^{-1}$) to 3.7 $\mu g_C\ L^{-1}$ in fresh snow (range 3.4–4.0 $\mu g_C\ L^{-1}$) to 2.9 $\mu g_C\ L^{-1}$ in wind drifts (range 2.5–3.9 $\mu g_C\ L^{-1}$) to 2.1 $\mu g_C\ L^{-1}$ in wind slabs (range 1.7–3.3 $\mu g_C\ L^{-1}$) to 1.5 $\mu g_C\ L^{-1}$ in depth hoar (0.7–2.6 $\mu g_C\ L^{-1}$). As with DOC, indurated depth hoars show the highest values, up to 110 $\mu g_C\ L^{-1}$. This increase is due to oxalic acid, whose concentration represents 80 to 95% of the carbon content of diacids in indurated depth hoar. Table 3 gives concentrations ranges in all the samples except indurated depth hoar, for the 3 measured diacids, as well as bivariate correlations between those concentrations. C4 and C5 diacids are well correlated, but none is correlated with oxalic, suggesting a distinct behavior for this last one. Figure 7 shows the contribution of diacids to DOC for various snow types. Except for diamond dust and indurated depth hoar that show respectively a lower (1.6%) and higher (4.6%) contribution to DOC, the contribution of diacids is stable, around a

Table 3. Concentration Range for Individual Diacids[a]

	Oxalic	Succinic	Glutaric
Concentrations (Min - Median - Max)	1.4–4.1–9.0	0.9–2.7–7.2	0.1–1.8–6.8
Correlations	[ox] = 0.06 [succ] + 4.2 (r^2 = 0.0025) [ox] = 0.09 [glut] + 4.1 (r^2 = 0.0041)	[succ] = 0.91 [glut] + 0.70 (r^2 = 0.63; $p < 0.0001$)	

[a]Indurated Depth Hoars are excluded from this analysis (see text). Concentrations in $\mu g.L^{-1}$.

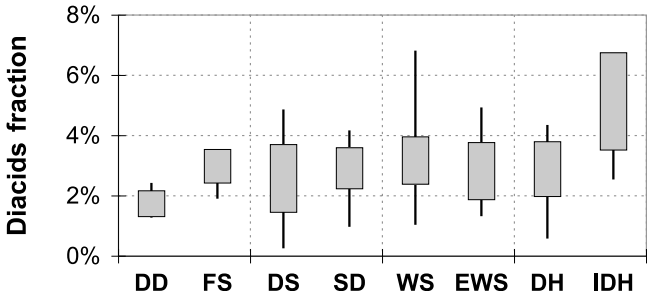

Figure 7. Box and whiskers plot of diacids contribution to DOC, for various snow types.

median value of 2.75% (half the values from 2% to 3.6%), pointing to different sources or processes for diamond dust and indurated depth hoar.

[41] Only 23 samples were analyzed for soluble HULIS, and these were all either diamond dust or fine grained snow types, with concentrations in the range 1 to 16 $\mu g_C.L^{-1}$, representing 2–15% of DOC. Based on those samples where we have data for aldehydes, diacids and soluble HULIS, we calculate that we classified only 5 to 20% of DOC (median value 8%) in Barrow. This clearly underlines how much DOC is unidentified. From 7 samples collected between March 4th and 9th from fine grained snow (drifting snow, blown snow and wind slab), we measured 1.5 to 1.8 $\mu g_C.L^{-1}$ from toluene, xylene and acetophenone, mostly from this last compound. This is indeed a small contribution to DOC (~1.5%). As it is on a very small set of species, it might be possible for VOCs as a whole to represent much more of the observed DOC. This clearly needs to be investigated further. Organochlorine were also tested for their contribution to DOC, but as expected for such compounds their cumulated concentrations formed a negligible contribution (7–600 $pg_C.L^{-1}$). Concentrations of only 4 individual aldehydes (formaldehyde, acetaldehyde, glyoxal and methylglyoxal) are used here. A few samples were also analyzed for hydroxyaldehyde, which was present at concentrations

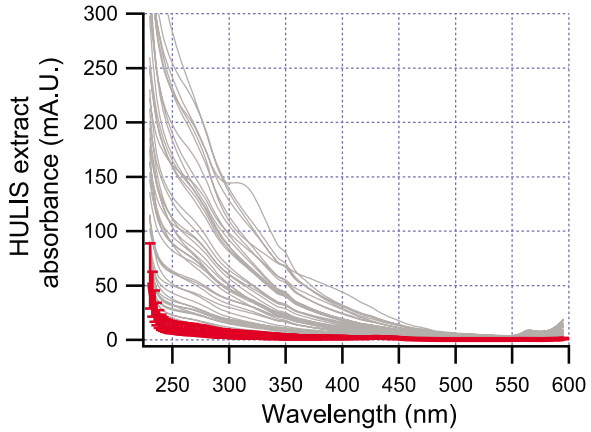

Figure 8. Raw absorption spectra for HULIS extracts. Blue line represents the average extraction blank, together with its variability (1 σ). Most extracts are very significantly above the extraction blank absorption. The increasing absorbance in blanks below 240 nm forbids any attempt at recovering useful data below 240 nm.

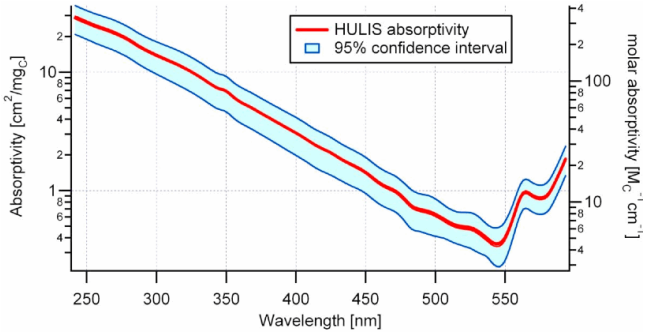

Figure 9. Average HULIS absorptivity at Barrow (red line). Left axis shows units per measured mg of carbon; right axis shows per mol C. The uncertainty, estimated at the 95% confidence level is ~30%.

comparable to what is reported for glyoxal. Also, traces of propionaldehyde and of other uncharacterized carbonyls were detected, which could contribute somewhat to reducing the gaping hole in the DOC budget, and should be better accounted for in the future.

4.3. Soluble HULIS Optical Properties

[42] Figure 8 shows the raw absorption spectra of soluble HULIS extracts, together with the absorption of the extraction blanks. The absorption of these blanks starts to increase significantly below 230 nm, precluding the recovery of soluble HULIS absorption below 240 nm. Yet, even with this high background, most extracts have absorptions that are very significantly above that of the extraction blanks above 240 nm. Using the measured carbon concentration in the extracts and the optical length of the cell, we calculated the base 10 soluble HULIS carbon mass absorptivity (in units of $cm^2\ mg_C^{-1}$), which is reported in Figure 9. The increase in absorptivity above 550 nm, clearly visible in the log scale, is responsible for the yellowish color of the extracts. The absorptivity at 250 nm is $A_{250} = 26 \pm 11\ cm^2\ mg_c^{-1}$ (or $310 \pm 130\ M_C^{-1}\ cm^{-1}$). This spectrum is typical for HULIS, showing a steep decrease with wavelength [e.g., *Baduel et al.*, 2010]. Table 4 shows the Angström Absorption Coefficients (AACs) calculated between several pairs of wavelength for the average soluble HULIS spectrum. Between 300 nm and 550 nm, the calculated AAC is 6.1, whereas it is only 4.5 between 300 and 350 nm, and raises to 7.7 between 450 and 500 nm. This dependence on wavelength of AAC is best viewed on Figure 10, which shows the one-wavelength AAC, as defined by *Moosmüller et al.*

Table 4. Angström Absorption Coefficients of the Average HULIS Spectrum, Calculated Between Different Pairs of Wavelengths, Indicated by the Line and Column Headers

	350 nm	400 nm	450 nm	500 nm	550 nm
300 nm	4.53	5.27	5.63	6.06	6.11
350 nm		6.09	6.29	6.71	6.66
400 nm			6.54	7.10	6.91
450 nm				7.72	7.14
500 nm					6.45

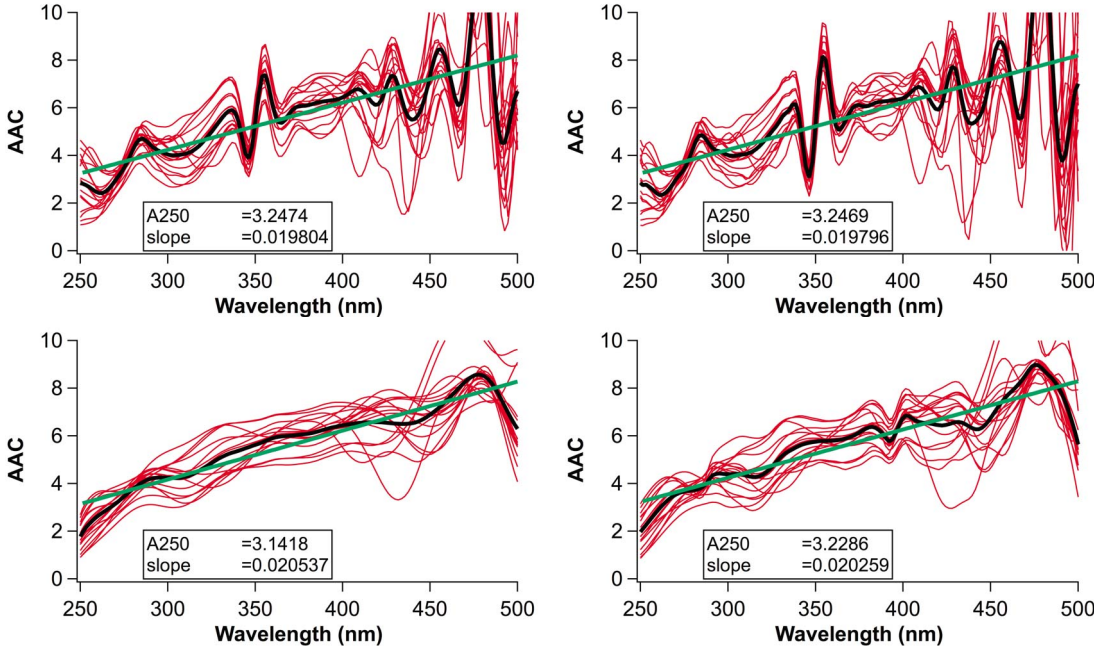

Figure 10. Wavelength-dependent Angström Absorption Coefficient for HULIS spectra, for different smoothing algorithms (running average on 3 and 11 points, left column; Savitsky-Golay on 11 and 51 points, right column). The average AAC (thick black line) is fitted with a line of equation AAC = A250 + slope $(\lambda - \lambda_0)$, where λ_0 = 250 nm.

[2011]. As expected from equation (3), many undulations appear in the AAC (see top line of Figure 10), corresponding to tiny shoulders in the absorption spectra of HULIS. Such features appear very consistently at 350 and 475 nm, and others appear around 425 and 450 nm, although not as consistently. A clear linear increase for AAC against wavelength is also visible, that does not depend much on the smoothing algorithm applied for the calculation, although the smoothing has a dramatic effect on the detailed shape of the average AAC.

5. Discussions

5.1. Soluble HULIS Concentrations, Optical Properties and Potential Sources

[43] Soluble HULIS is an operationally defined carbon pool. The extraction method used here extracts polyacidic species [*Baduel et al.*, 2009], while excluding dicarboxylic acids with a carbon chain up to 7 carbon atoms. Species such as sugars and phenols are also excluded, which is not necessarily true for other extraction schemes. Comparing different extraction schemes for soluble HULIS on aerosol shows that the measured concentrations can differ by up to a factor three [*Lukács et al.*, 2007; *Baduel et al.*, 2009] Comparisons must therefore be made with caution. Measurements of soluble HULIS, and more generally humic or fulvic acids are very few in snow samples. Some pioneering work showed the presence of soluble fulvic acids in Antarctica surface snow, extracted from very high volumes by standard protocols as defined by the International Humic Substances Society [*Calace et al.*, 2001, 2005]. The same protocols have been used to extract soluble HULIS from aerosols [*Dinar et al.*, 2006, 2007, 2008], and these measurements can thus be compared to ours. The measured concentrations (20–220 $\mu g.L^{-1}$) are about 15 times higher than our own measurements, which is higher than expected only from using a different extraction scheme. Sources of organic material are expected to be much smaller in Antarctic compared to the Arctic: carboxylic acid concentrations are an order of magnitude higher in Holocene ice from central Greenland than from coastal East Antarctica [*Legrand and De Angelis*, 1995]. Unless the relative concentrations of carboxylic acid and soluble HULIS are wildly different in Antarctica versus the Arctic, there should be more soluble HULIS in our coastal samples (Barrow) than in samples from inland Antarctica (10 to 400 km, between Mario Zuccheli and Concordia stations). *Legrand et al.* [2007a] measured soluble HULIS concentrations in an Alpine ice core in the range 50 to 400 $\mu g_C\ L^{-1}$, which amounted to about half of DOC. However, the analytical method used, based on UV absorbance of soluble HULIS, was highly imprecise, measuring on some samples more soluble HULIS than the observed DOC concentration; again, further comparison is difficult.

[44] There are no previous direct measurements of soluble HULIS available for Arctic snow; yet, some indirect assessment can be made, first on insoluble HULIS, from measurements on WinOC. *Grannas et al.* [2004] showed from samples from Alert that ~5% of WinOC was degraded lignin. This vegetation source, upon degradation, should contribute to total (soluble and insoluble) HULIS in the snow, giving a lower estimate of total HULIS content of a few $ng.g^{-1}$, in good agreement with our own measurements for a similar environment. The recently published survey of absorbing insoluble species in arctic snow [*Doherty et al.*, 2010] clearly shows, from spectrally resolved absorption of

the insoluble content of the snow, the presence of some absorbing species besides Black Carbon. This could be related to absorbing carbon such as insoluble HULIS or to dust. The difference between their estimated Black Carbon and maximum Black Carbon concentrations can be used as a proxy for insoluble HULIS. As dust can also contribute to the absorption besides BC, this approach may overestimate insoluble HULIS. This estimate gives about 1 to 10 $ng_C.g^{-1}$ insoluble HULIS in arctic snow, in good agreement with the value estimated from *Grannas et al.* [2004]. Last, based on observations from aerosols [*Havers et al.*, 1998; *Feczko et al.*, 2007; *Baduel et al.*, 2009, 2011] we make the assumption that the soluble and insoluble fractions of HULIS are of similar magnitude, and estimate from those previous measurements 1 to 10 $ng_C.g^{-1}$ soluble HULIS in arctic snow, which agrees well with our own measurements.

[45] The absorption spectra measured here (Figure 9) have been used by *Beine et al.* [2011] to show that soluble HULIS are responsible for half of the integrated absorption of water soluble compounds in snow in the photochemically active region (300–450 nm). This makes HULIS a probable key to the understanding of snowpack photochemistry and stresses the necessity to understand their sources and spectral features.

[46] The measured soluble HULIS spectrum essentially shows a decrease with wavelength usual for this kind of extracts [e.g., *Baduel et al.*, 2009, 2010]. The slope of the spectrum, as given by the AAC (Figure 10) shows a linear increasing trend with wavelength, with equation AAC = $3.24 + 0.02\ (\lambda - 250)$. This trend is quite robust, as it does not depend on the specifics of the smoothing algorithm chosen and also exists when calculating the AAC from the raw HULIS spectra. This is in contrast with previous studies on equivalent systems that show either a constant AAC [*Hecobian et al.*, 2010], or AAC decreasing with wavelength [*Chen and Bond*, 2010], and remains to be explained. As seen in the top line of Figure 10, the one wavelength AAC, as proposed by *Moosmüller et al.* [2011] also reveals specific spectral features: shoulders at 350, 425, 450 and 475 nm. These are barely visible on the absorbance spectrum where only the general decreasing slope and the stub of a peak starting above 550 nm appear. The features above 400 nm are very similar to what is observed on chlorophyll and carotenoid containing extracts from plant leaves and sea surface [*Bricaud et al.*, 1995; *Chappelle et al.*, 1992].

[47] *Baduel et al.* [2010] used simpler spectral features of soluble HULIS to discuss their sources in the aerosol for urban sites in the Alps. They showed that absorptivity at 250 nm (A_{250}) presents a strong seasonal cycle, going from $22.6 \pm 4.5\ cm^2\ mg_C^{-1}$ in summer to $42.3 \pm 6.0\ cm^2\ mg_C^{-1}$ in winter. This seasonal difference was related to structural differences in soluble HULIS due to a shift in sources: winter soluble HULIS, produced by biomass burning, are more aromatic; summer soluble HULIS, produced by the atmospheric processing of VOCs, are more aliphatic. Both winter and summer soluble HULIS were less absorptive than standard fulvic (Suwanee River Fulvic Acid: $A_{250} = 52\ cm^2\ mg_C^{-1}$) or humic acids (Fluka: $A_{250} = 72\ cm^2\ mg_C^{-1}$). Soluble HULIS in Barrow snow have a specific absorbance very close to summer aerosol soluble HULIS from the Alps ($A_{250} = 26 \pm 11\ cm^2\ mg_c^{-1}$), i.e., significantly lower than both biomass burning soluble HULIS and regular fulvic or humic acids. A_{250} is not very specific, and other spectral features are needed to further characterize soluble HULIS: A_{250}/A_{340} is commonly used as an indicator of aromaticity for aquatic fulvic acids [*Peuravuori and Pihlaja*, 1997], and for soluble HULIS [*Duarte et al.*, 2005; *Krivácsy et al.*, 2008]. This indicator increases with decreasing aromaticity. For our soluble HULIS, we measure $A_{250}/A_{340} = 3.7 \pm 1.4$, to be compared with 3.1–3.5 observed by *Baduel et al.* [2010] in winter (biomass burning), and 4.5–6 in summer (secondary production). Therefore, Barrow's soluble HULIS are slightly less aromatic than urban biomass burning aerosol, and much more aromatic than secondary aerosol soluble HULIS. Our observations could be explained by soluble HULIS originating from long range transport of biomass burning plumes: *Baduel et al.* [2011] observed in controlled photochemical aging experiments that biomass burning HULIS become less absorptive through photolysis and reaction with O_3. An alternative explanation could also be a third source for soluble HULIS, with an aromaticity similar to that of urban biomass burning aerosol soluble HULIS, together with a lower specific absorbance. Such a source would need to be optically characterized, but could be of marine origin. *Domine et al.* [2011] suggest that exopolysaccharides (EPS) biogels originating from the surface microlayer of open leads are a major contributor to the large DOC concentrations observed in diamond dust; such a source would most likely also provide some soluble HULIS material, as observed by *Cavalli et al.* [2004] over the North Atlantic. Furthermore, such origin would also fit with the presence of peaks at 425, 450, 475 nm and the general increase between 500 and 600 nm that suggest the presence of chlorophyll and carotenoid such as found in surface ocean phytoplankton [*Bricaud et al.*, 1995]. Further investigations are needed to confirm the marine origin of soluble HULIS in Barrow snow, but the suggestion deserves consideration.

5.2. Snowpack Formation, Physical Evolution and Links With Chemistry

[48] Snow physics interactions with chemical composition are illustrated in Figure 1. Displaying snow composition as a function of snow type provides a unique opportunity to discuss the influence of snow physical properties on snow chemical composition. When looking at Figures 4 and 6, indurated depth hoar stands out as the type of snow with the highest DOC. We will see that it can be linked to its formation process at the early stages of the snow season (section 5.2.1). In other snow types, DOC decreases from freshest to oldest snow, i.e., from diamond dust to depth hoar through remobilized snow and wind slabs (section 4 above; Figures 4 and 6). This decrease will be linked to the processes illustrated in Figure 1.

5.2.1. Early Season Snowpack Processes and Depth Hoar Chemical Composition

[49] Depth hoar is present as indurated depth hoar (IDH) or soft depth hoar (DH). These two types of snow have radically different chemical composition relative to each other and relative to fine grain snows (wind slabs and remobilized snow). Especially, DH is depleted in DOC, whereas IDH is enriched in DOC and conservative ions (ions that cannot be released from the snowpack as a gas, nor be formed by gas phase reactivity, see Table 5 and Figure 4). This difference can be related to the formation history of

Table 5. Concentration Range, Given as First Quartile Minus Third Quartile (Median) for Major Conservative Ions in Depth Hoar (DH), Indurated Depth Hoar (IDH) and Surface Snows (Wind Slabs and Remobilized Snow)[a]

	Na^+	Mg^{2+}	Ca^{2+}	K^+
DH	0.9–6.5 (3.6)	0.2–1.4 (0.7)	0.1–0.6 (0.3)	0.03–0.2 (0.1)
IDH	19–48 (30)	3.7–11 (8.3)	1.4–4.1 (3.9)	0.7–2.6 (1.3)
Surface Snow	2.0–6.0 (4.2)	0.6–1.6 (0.9)	0.3–0.9 (0.4)	0.1–0.34 (0.16)

[a]Concentrations in mg L^{-1}.

IDH and DH. Both are formed by snow metamorphism under a high temperature gradient, starting from different initial snow: IDH forms from a wind slab, whereas soft DH forms from light non-packed snow. This leads to the following scenario.

[50] At the beginning of the season, a fresh snowfall is wind-blown. There is still a significant fraction of the ground that is exposed. Therefore, a lot of dust, soil, and vegetal debris are mixed in with the snow. This is why this basal drift snow may have high OC and ions concentrations. It may also look dirty. It will then sinter, form a hard wind slab, with a typical density around 350 kg m^{-3}. Because of the strong temperature gradient (TG) between the ground that is still warm and the already cold atmosphere, mass loss by sublimation will take place and IDH will form, even though the snow is denser than what was often thought as the upper density limit for DH formation [*Marbouty*, 1980]. Some parts of the IDH remain unaffected by DH formation, which is why small grains remain and IDH should look whiter than DH [*Domine et al.*, 2012], for the same hypothetical content in impurities. On the other hand, if a snow fall is barely wind-blown and its density remains <250 kg m^{-3}, it will turn into DH. Since it is less wind-blown than the wind slab that gave birth to IDH, less dust and vegetal debris will be incorporated into it, leading to the observed difference in concentrations in those two types of snow.

[51] There are therefore two factors that will determine DH impurity content: (1) Did it form from a wind slab or from unremobilized fresh snow? (2) How close to the ground is it, i.e., what was the snow fractional cover when it formed? Normally, there is little relationship between height above ground and IDH/DH formation, although IDH is less likely to form higher up in the snowpack, i.e., later in the season, because the lower temperature gradients that then prevail reduce the likelihood that a wind slab will be transformed into IDH. In any case, what determines whether an early season snowfall will turn into IDH or DH is mostly the coincidence between wind events and precipitation. Visual observation during the campaign indicates that blowing snow occurred when wind speed exceeded 5–7 m s^{-1} [*Domine et al.*, 2012]. In 2009, early snowfalls were affected by wind, while later ones less so. Data from the NOAA observatory near our sampling site (http://www.esrl.noaa.gov/gmd/dv/data/?category = Meteorology&site = brw) shows that wind speeds at 10 m height exceeded 6 m s^{-1} 46% (56%) of the time in October (November), and 33% (25%) in December (January). This need not be a general trend, but highlights the importance of meteorological conditions at the onset of the snow season to explain the overall carbon load in the snowpack.

[52] It should be stressed here that snowpack erosion can expose these deep IDH layers, as can be seen in Figure 3. These carbon rich layers typically covered 5–10% of the landscape around our sampling site and are especially interesting in terms of atmospheric interactions, because their high absorber content and high e-folding depth for that amount of absorber (due to the large crystals) ensures very active photochemistry, and their high permeability [*Domine et al.*, 2008] ensures easy ventilation and release of photochemical VOCs.

5.2.2. Diamond Dust and Fine Grain Snow

[53] Diamond dust has a very specific chemical composition compared to fine grain snow or fresh snow: higher concentrations in DOC, aldehydes, diacids than surface snows (Figure 4), but lower HULIS / DOC, diacids / DOC, aldehydes / DOC ratios (Table 6). *Domine et al.* [2011] detail this specific chemical signature, and attribute it to exopolysaccharide (EPS) biogels dominating the diamond dust chemical composition. EPS biogels are neutral molecules, and will not be isolated as HULIS, and they are neither aldehydes nor diacids: their high contribution to DOC in diamond dust would explain our observation of a lower contribution for HULIS, aldehydes and diacids. *Barret et al.* [2011b], through a very careful examination of formaldehyde time series, show that recently deposited DD is a photoactive layer producing formaldehyde, glyoxal, methylglyoxal, and probably many other molecules that they did not analyze. Formaldehyde gets mostly emitted to the atmosphere, whereas methylglyoxal and glyoxal are stored in the snow layer. They also show that reemission to the atmosphere of the formaldehyde that has been stored in the snow occurs during snow remobilization by the wind, through snow crystal sublimation.

[54] We observe a relative enrichment in non-volatile species (dicarboxylics, HULIS; see Table 6) going from diamond dust to fine grain snow, which would imply some preferential loss of volatiles from the DOC pool. This seems in contradiction with having DOC in the diamond dust enriched by non-volatile EPS biogels. And at the same time, the non-volatile diacids decrease from DD to surface snows, implying some photochemical losses. A possible explanation would imply fast fragmenting chemistry for EPS biogels, leading to products volatile enough to be as efficiently re-equilibrated as formaldehyde.

5.2.3. Depth Hoar Formation and Carbon Loss Processes

[55] The second largest loss of DOC is between wind slabs and depth hoar layers. In Barrow, the depth hoar layers usually sit under 10 to 20 cm thick wind slabs. At such depth, photolysis rates for H_2O_2, NO_3^- and NO_2^- are reduced

Table 6. Fraction of DOC Explained by the Identified Fractions for Diamond Dust and Fine Grained Snows

	HULIS/DOC (%)	Diacids/DOC (%)	Aldehydes/DOC (%)
Diamond Dust	3–4	1–2	0.8–1.3
Wind slabs	4–10	2–4	2–8

by at least 1 or 2 orders of magnitude [*France et al.*, 2012], and so are the possibilities for oxidative photochemistry: DOC decrease must be either from physical equilibrium or from gravitational settling. Chemically inert species would be affected only by gravitational settling. Such species include EC, for which we do not have enough data on depth hoar to conclude. Other potential test species include non-volatile ions, such as Ca^{2+}, Mg^{2+}, Na^{+} and K^{+}. Table 5 shows that all these species present 15–35% loss between wind slabs and depth hoar, which should be attributed to gravitational settling. We observe 53% losses for DOC between wind slabs and depth hoar. Even taking into account that part of the loss can be from gravitational settling, it leaves 20–40% of the losses mostly related to thermochemical equilibrium. This can either be from species adsorbed at the surface of snow grains that get reemitted as the specific surface area decreases [*Taillandier et al.*, 2006], or from species embedded within snow crystals, and whose partition changes as water vapor gets massively remobilized when depth hoar forms [see [*Pinzer and Schneebeli*, 2009].

5.2.4. Fine Grained Snow and Photochemical Transformations

[56] When concentrating on fine grain snow, we observe that the relative contribution of non-volatiles (dicarboxylics) to DOC stays approximately constant (Figure 7). Dicarboxylic acids are essentially non-volatile [*Booth et al.*, 2010], and thus the decrease of their concentration as snow ages has to be from photochemistry in the snowpack, as well as for DOC.

[57] Glutaric and succinic acids are well correlated (see Table 3), which suggests a common chemistry. Oxalic is uncorrelated to either of them, suggesting at least partially different processes. *Narukawa et al.* [2002] observed in Alert that whereas oxalic acid concentrations didn't evolve much in aerosol and surface snow from winter to spring, glutaric and succinic concentrations increased significantly. Postulating common precursors for all the diacids, brought to the Arctic by long range transport, they explained the absence of oxalic acid increase by an additional reactivity, possibly linked to bromine chemistry. *Legrand et al.* [2007b] measured a suite of diacids in European aerosol, and also found glutaric and succinic to be well correlated, but less so with oxalic acid. They interpreted that in terms of the production mechanism suggested by *Ervens et al.* [2004]: diacids, from azelaic (C6) down to oxalic (C2), derive from each other by successive decarboxylation due to OH reactivity in liquid clouds. This chemical mechanism [see *Legrand et al.*, 2007b, Figure 2] induces the observed correlations, to which oxalic partly escapes because of a parallel production mechanism involving glyoxal and methylglyoxal, also in cloud water.

[58] Building upon this idea, we consider that a similar photochemistry could be occurring in the snowpack, as liquid water does not directly intervene in Ervens' proposed mechanism, and only act through the stabilizing hydration shell it provides to carbonyl groups. OH radicals are known to be produced in the snowpack by photolysis of H_2O_2 and NO_3^- [*Anastasio et al.*, 2007]. Successive decarboxylation of diacids would over time decrease their concentrations, while maintaining the observed correlation between glutaric and succinic acid. The presence of glyoxal and methylglyoxal, probably produced in the snowpack from marine precursors [*Domine et al.*, 2011], would provide an independent source of oxalic acid. Bromine chemistry, which is active in the snowpack in spring, would independently destroy oxalic acid, as suggested by *Narukawa et al.* [2002], and explain the absence of correlation between oxalic and the other diacids. More detailed time series of diacids and aldehydes concentrations in the snow, as well as a better identification of possible precursors, would be necessary to further test this hypothesis.

5.2.5. Carbon Reemission to the Atmosphere

[59] Overall, our observations indicate that DOC deposited with fresh precipitation is partly reemitted to the atmosphere during snow metamorphism, either by photochemical degradation or by physical equilibration. To estimate the importance of those losses, we need to compare the integrated amount of carbon in the snowpack to an estimated initial amount. The integrated amount of carbon can be estimated from a simplified stratigraphy and our measured DOC concentrations. The simplified stratigraphy contains three layers: depth hoar (20 cm), wind slab (11.4 cm) and wind drift (10 cm). It contains no indurated depth hoar, as DOC in this snow type has a specific origin (soils, by wind mobilization in the early season). The total height is the average snow depth measured near Barrow (41.4 cm [*Domine et al.*, 2012]). Using the average observed density (300 $kg.m^{-3}$) and the measured median DOC for each snow type, we calculate that the snowpack in Barrow contains 1.0 $\mu g_C\ cm^{-2}$ DOC. Over an entire season, the various snow falls will have different chemical compositions. As we only sampled diamond dust and fresh snow from a few specific events, evaluating an initial state to compare with is somewhat difficult. We assume three initial snowpacks: diamond dust (4.0 $\mu g_C\ cm^{-2}$), fresh snow (1.7 $\mu g_C\ cm^{-2}$), wind drift (1.4 $\mu g_C\ cm^{-2}$). The first most probably overestimates initial DOC content, whereas the other two most probably underestimate it. The estimated losses range from 31 to 76% (41% for fresh snow). Assuming those losses occur only during daytime (140 cumulated hours from October 1st to February 14th), the corresponding carbon flux from the snow to the atmosphere ranges from 30 to 220 $\mu g_C\ m^{-2}\ h^{-1}$.

[60] This calculated carbon flux includes photochemical productions of CO and CO_2 and should thus be corrected to estimate a VOC flux. *Goldstein and Galbally* [2007] estimated that 20–40% of the VOCs gas phase oxidation produces CO or CO_2. For lack of a similar estimate for organic aerosol oxidation, and because emissions from organics in the snow will also go through some gas phase oxidation in the interstitial air, we choose to use the same estimate to correct for CO and CO_2 emissions. This leads to an estimated 20 to 170 $\mu g_C\ m^{-2}\ h^{-1}$ VOC flux out of the snow from photochemical oxidation of organic carbon in the snow. *Flocke et al.* [2011], based on a photochemical box model, estimated formaldehyde and acetaldehyde emission fluxes to the atmosphere during ozone depletion events in Barrow, and found 6.0 $\mu g_C\ m^{-2}\ h^{-1}$. *Boudries et al.* [2002] also estimated snow to atmosphere fluxes of acetaldehyde, acetone and methanol during the ALERT2000 field campaign, and found a total carbon flux of 5.6 $\mu g_C\ m^{-2}\ h^{-1}$. Our calculated flux is only 10 times higher than these two

estimates, suggesting larger emissions of VOCs from the snow to the atmosphere than previously estimated.

6. Conclusions

[61] In this study, we built a data set of snow chemical composition and physical properties, to be used in future photochemistry modeling studies. This data set includes snow type, as a marker of snow metamorphic history, as well as chemical composition of the carbonaceous fraction: Elemental Carbon (EC), Water insoluble Organic Carbon (WinOC), Dissolved Organic Carbon (DOC) and Total Carbon Content (TCC = EC+WinOC+DOC). DOC is further speciated in aldehydes, dicarboxylic acids, and for selected samples HULIS and some VOCs.

[62] TCC is found to range from 100 to 400 $\mu g_C.L^{-1}$ in rounded grain snows found in the upper part of the snowpack, with values somewhat higher in blowing or recently blown snow compared to older wind slabs, which is interpreted as a sign of carbon loss as snow ages. EC represent only a minor fraction (<5%), and WinOC a very significant fraction (28–42%) of TCC. Also, DOC was measured in precipitating snow (Fresh Snow and Diamond Dust) and in two types of depth hoar layers. DOC was higher in fresh snow than in rounded grain snows, and still higher in diamond dust. DOC was found to be highest in indurated depth hoars and lowest in regular depth hoar.

[63] The very high concentrations observed in indurated depth hoar were traced to soil input by high winds in the early season, when the snow cover is still incomplete on the ground. Although this mechanism is very specific to certain snow layers, it is suggested that it may be important for the overall snowpack chemistry: these old layers can be later exposed to the atmosphere by snow erosion, and represent typically 10% of the surface around Barrow. Overall, this source is the most important source of carbon to the snowpack in Barrow.

[64] These indurated depth hoar layers set apart, we observed a decrease in DOC going from diamond dust to fresh snow to remobilized snow to wind slabs to depth hoar, furthering the observation on TCC. Depending on the relative contributions of diamond dust and fresh snow to the overall seasonal snowpack, we estimate that 31 to 76% of the carbon deposited to the snow from the atmosphere is eventually released back to the boundary layer, either from photochemical reactions in the upper layers or from physical re-equilibration at the formation of depth hoar. Assuming a purely photochemical flux, we estimate an upper limit for the VOC flux of 20 to 170 $\mu g_C\ m^{-2}\ h^{-1}$.

[65] Soluble HULIS concentrations vary from 1 to 16 $\mu g_C.L^{-1}$, representing 2–15% of DOC. Their absorption spectra were measured and used to infer possible sources. Aromaticity and specific absorbance at 250 nm suggest aged biomass burning as a possible source for this light absorbing carbon. Other specific spectral features suggest ocean phytoplankton as an possible additional source. Overall, measured aldehydes, dicarboxylic acids and soluble HULIS only represented 5 to 20% of DOC, meaning that further developments and characterization are needed to fully understand the chemical properties of snowpacks.

[66] **Acknowledgments.** The participation of D.V., F.D., S.H. and M.B. to the Barrow field campaign was funded by the French Polar Institute (IPEV) grant 1017 to F.D. and by the National Science Foundation, through grant ATM-0807702 to H.B. Part of the analysis in Grenoble was funded by INSU – LEFE CHAT. Participation of A.G. was funded by the National Science Foundation (ATM-0547435).

References

Anastasio, C., and T. Robles (2007), Light absorption by soluble chemical species in Arctic and Antarctic snow, *J. Geophys. Res.*, *112*, D24304, doi:10.1029/2007JD008695.

Anastasio, C., E. S. Galbavy, M. A. Hutterli, J. F. Burkhart, and D. K. Friel (2007), Photoformation of hydroxyl radical on snow grains at Summit, Greenland, *Atmos. Environ.*, *41*(24), 5110–5121, doi:16/j.atmosenv.2006.12.011.

Baduel, C., D. Voisin, and J. L. Jaffrezo (2009), Comparison of analytical methods for Humic Like Substances (HULIS) measurements in atmospheric particles, *Atmos. Chem. Phys.*, *9*(16), 5949–5962, doi:10.5194/acp-9-5949-2009.

Baduel, C., D. Voisin, and J. Jaffrezo (2010), Seasonal variations of concentrations and optical properties of water soluble HULIS collected in urban environments, *Atmos. Chem. Phys.*, *10*(9), 4085–4095, doi:10.5194/acp-10-4085-2010.

Baduel, C., D. Voisin, J. Jaffrezo, M. E. Monge, B. D'Anna, C. George, I. El Haddad, and N. Marchand (2011), Oxidation of atmospheric Humic like substances by ozone: A kinetic and structural analysis approach, *Environ. Sci. Technol.*, *45*(12), 5238–5244, doi:10.1021/es200587z.

Barret, M., S. Houdier, and F. Domine (2011a), Thermodynamics of the formaldehyde-water and formaldehyde-ice systems for atmospheric applications, *J. Phys. Chem. A*, *115*(3), 307–317, doi:10.1021/jp108907u.

Barret, M., F. Dominé, S. Houdier, J. Gallet, P. Weibring, J. Walega, A. Fried, and D. Richter (2011b), Formaldehyde in the Alaskan Arctic snowpack: Partitioning and physical processes involved in air-snow exchanges, *J. Geophys. Res.*, *116*, D00R03, doi:10.1029/2011JD016038.

Bartels-Rausch, T., M. Brigante, Y. F. Elshorbany, M. Ammann, B. D'Anna, C. George, K. Stemmler, M. Ndour, and J. Kleffmann (2010), Humic acid in ice: Photo-enhanced conversion of nitrogen dioxide into nitrous acid, *Atmos. Environ.*, *44*(40), 5443–5450, doi:10.1016/j.atmosenv.2009.12.025.

Beine, H. J., A. Amoroso, F. Dominé, M. D. King, M. Nardino, A. Ianniello, and J. L. France (2006), Surprisingly small HONO emissions from snow surfaces at Browning Pass, Antarctica, *Atmos. Chem. Phys.*, *6*(9), 2569–2580, doi:10.5194/acp-6-2569-2006.

Beine, H., A. J. Colussi, A. Amoroso, G. Esposito, M. Montagnoli, and M. R. Hoffmann (2008), HONO emissions from snow surfaces, *Environ. Res. Lett.*, *3*(4), 045005, doi:10.1088/1748-9326/3/4/045005.

Beine, H. J., C. Anastasio, G. Esposito, K. Patten, E. Wilkening, F. Dominé, D. Voisin, M. Barret, S. Houdier, and S. Hall (2011), Soluble, light-absorbing species in snow at Barrow, Alaska, *J. Geophys. Res.*, *116*, D00R05, doi:10.1029/2011JD016181.

Booth, A. M., M. H. Barley, D. O. Topping, G. McFiggans, A. Garforth, and C. J. Percival (2010), Solid state and sub-cooled liquid vapour pressures of substituted dicarboxylic acids using Knudsen Effusion Mass Spectrometry (KEMS) and Differential Scanning Calorimetry, *Atmos. Chem. Phys.*, *10*(10), 4879–4892, doi:10.5194/acp-10-4879-2010.

Boudries, H., J. W. Bottenheim, C. Guimbaud, A. M. Grannas, P. B. Shepson, S. Houdier, S. Perrier, and F. Domine (2002), Distribution and trends of oxygenated hydrocarbons in the high Arctic derived from measurements in the atmospheric boundary layer and interstitial snow air during the ALERT2000 field campaign, *Atmos. Environ.*, *36*(15–16), 2573–2583, doi:10.1016/S1352-2310(02)00122-X.

Bricaud, A., M. Babin, A. Morel, and H. Claustre (1995), Variability in the chlorophyll-specific absorption coefficients of natural phytoplankton: Analysis and parameterization, *J. Geophys. Res.*, *100*(C7), 13,321–13,332, doi:10.1029/95JC00463.

Brock, C. A., et al. (2011), Characteristics, sources, and transport of aerosols measured in spring 2008 during the aerosol, radiation, and cloud processes affecting Arctic Climate (ARCPAC) Project, *Atmos. Chem. Phys.*, *11*(6), 2423–2453, doi:10.5194/acp-11-2423-2011.

Calace, N., B. M. Petronio, R. Cini, A. M. Stortini, B. Pampaloni, and R. Udisti (2001), Humic marine matter and insoluble materials in Antarctic snow, *Int. J. Environ. Anal. Chem.*, *79*(4), 331–348, doi:10.1080/03067310108044393.

Calace, N., E. Cantafora, S. Mirante, B. M. Petronio, and M. Pietroletti (2005), Transport and modification of humic substances present in Antarctic snow and ancient ice, *J. Environ. Monit.*, *7*(12), 1320–1325, doi:10.1039/b507396k.

Cavalli, F., et al. (2004), Advances in characterization of size-resolved organic matter in marine aerosol over the North Atlantic, *J. Geophys. Res.*, *109*, D24215, doi:10.1029/2004JD005137.

Cavalli, F., M. Viana, K. E. Yttri, J. Genberg, and J.-P. Putaud (2010), Toward a standardised thermal-optical protocol for measuring atmospheric organic and elemental carbon: The EUSAAR protocol, *Atmos. Meas. Tech.*, *3*(1), 79–89, doi:10.5194/amt-3-79-2010.

Chappelle, E. W., M. S. Kim, and J. E. McMurtrey III (1992), Ratio analysis of reflectance spectra (RARS): An algorithm for the remote estimation of the concentrations of chlorophyll a, chlorophyll b, and carotenoids in soybean leaves, *Remote Sens. Environ.*, *39*(3), 239–247, doi:10.1016/0034-4257(92)90089-3.

Chebbi, A., and P. Carlier (1996), Carboxylic acids in the troposphere, occurrence, sources, and sinks: A review, *Atmos. Environ.*, *30*(24), 4233–4249, doi:16/1352-2310(96)00102-1.

Chen, Y., and T. C. Bond (2010), Light absorption by organic carbon from wood combustion, *Atmos. Chem. Phys.*, *10*(4), 1773–1787, doi:10.5194/acp-10-1773-2010.

Chu, L., and C. Anastasio (2003), Quantum yields of hydroxyl radical and nitrogen dioxide from the photolysis of nitrate on ice, *J. Phys. Chem. A*, *107*(45), 9594–9602, doi:10.1021/jp0349132.

Decesari, S., M. C. Facchini, E. Matta, F. Lettini, M. Mircea, S. Fuzzi, E. Tagliavini, and J.-P. Putaud (2001), Chemical features and seasonal variation of fine aerosol water-soluble organic compounds in the Po Valley, Italy, *Atmos. Environ.*, *35*(21), 3691–3699, doi:10.1016/S1352-2310(00)00509-4.

Dinar, E., T. F. Mentel, and Y. Rudich (2006), The density of humic acids and humic like substances (HULIS) from fresh and aged wood burning and pollution aerosol particles, *Atmos. Chem. Phys.*, *6*(12), 5213–5224, doi:10.5194/acp-6-5213-2006.

Dinar, E., I. Taraniuk, E. R. Graber, T. Anttila, T. F. Mentel, and Y. Rudich (2007), Hygroscopic growth of atmospheric and model humic-like substances, *J. Geophys. Res.*, *112*, D05211, doi:10.1029/2006JD007442.

Dinar, E., A. A. Riziq, C. Spindler, C. Erlick, G. Kiss, and Y. Rudich (2008), The complex refractive index of atmospheric and model humic-like substances (HULIS) retrieved by a cavity ring down aerosol spectrometer (CRD-AS), *Faraday Discuss.*, *137*, 279–295, doi:10.1039/b703111d.

Doherty, S. J., S. G. Warren, T. C. Grenfell, A. D. Clarke, and R. E. Brandt (2010), Light-absorbing impurities in Arctic snow, *Atmos. Chem. Phys.*, *10*(23), 11,647–11,680, doi:10.5194/acp-10-11647-2010.

Domine, F., and P. B. Shepson (2002), Air-snow interactions and atmospheric chemistry, *Science*, *297*(5586), 1506–1510, doi:10.1126/science.1074610.

Domine, F., A. Cabanes, and L. Legagneux (2002), Structure, microphysics, and surface area of the Arctic snowpack near Alert during the ALERT 2000 campaign, *Atmos. Environ.*, *36*(15–16), 2753–2765, doi:16/S1352-2310(02)00108-5.

Domine, F., R. Sparapani, A. Ianniello, and H. J. Beine (2004), The origin of sea salt in snow on Arctic sea ice and in coastal regions, *Atmos. Chem. Phys.*, *4*(9/10), 2259–2271, doi:10.5194/acp-4-2259-2004.

Domine, F., A. Cincinelli, E. Bonnaud, T. Martellini, and S. Picaud (2007), Adsorption of phenanthrene on natural snow, *Environ. Sci. Technol.*, *41*(17), 6033–6038, doi:10.1021/es0706798.

Domine, F., M. Albert, T. Huthwelker, H. Jacobi, A. A. Kokhanovsky, M. Lehning, G. Picard, and W. R. Simpson (2008), Snow physics as relevant to snow photochemistry, *Atmos. Chem. Phys.*, *8*(2), 171–208, doi:10.5194/acp-8-171-2008.

Domine, F., J.-C. Gallet, M. Barret, S. Houdier, D. Voisin, T. A. Douglas, J. D. Blum, H. J. Beine, C. Anastasio, and F.-M. Bréon (2011), The specific surface area and chemical composition of diamond dust near Barrow, Alaska, *J. Geophys. Res.*, *116*, D00R06, doi:10.1029/2011JD016162.

Domine, F., J.-C. Gallet, J. Bock, and S. Morin (2012), Structure, specific surface area and thermal conductivity of the snowpack around Barrow, Alaska, *J. Geophys. Res.*, *117*, D00R14, doi:10.1029/2011JD016647.

Duarte, R. M., C. A. Pio, and A. C. Duarte (2005), Spectroscopic study of the water-soluble organic matter isolated from atmospheric aerosols collected under different atmospheric conditions, *Anal. Chim. Acta*, *530*(1), 7–14, doi:10.1016/j.aca.2004.08.049.

Ducret, J., and H. Cachier (1992), Particulate carbon content in rain at various temperate and tropical locations, *J. Atmos. Chem.*, *15*(1), 55–67, doi:10.1007/BF00053609.

Ervens, B., G. Feingold, G. J. Frost, and S. M. Kreidenweis (2004), A modeling study of aqueous production of dicarboxylic acids: 1. Chemical pathways and speciated organic mass production, *J. Geophys. Res.*, *109*, D15205, doi:10.1029/2003JD004387.

Feczko, T., H. Puxbaum, A. Kasper-Giebl, M. Handler, A. Limbeck, A. Gelencsér, C. Pio, S. Preunkert, and M. Legrand (2007), Determination of water and alkaline extractable atmospheric humic-like substances with the TU Vienna HULIS analyzer in samples from six background sites in Europe, *J. Geophys. Res.*, *112*, D23S10, doi:10.1029/2006JD008331.

Flanner, M. G., C. S. Zender, P. G. Hess, N. M. Mahowald, T. H. Painter, V. Ramanathan, and P. J. Rasch (2009), Springtime warming and reduced snow cover from carbonaceous particles, *Atmos. Chem. Phys.*, *9*(7), 2481–2497, doi:10.5194/acp-9-2481-2009.

Flocke, F. M., et al. (2011), Gas-phase photochemistry during the 2009 OASIS Barrow Field Intensive, Abstract A12D-04 presented at 2011 Fall Meeting, AGU, San Francisco, Calif., 5–9 Dec.

France, J. L., H. J. Reay, M. D. King, D. Voisin, H. Jacobi, H. J. Beine, C. Anastasio, A. MacArthur, and J. Lee-Taylor (2012), Hydroxyl radical and NO_x production rates, black carbon concentrations and light-absorbing impurities in snow from field measurements of light penetration and nadir reflectivity of on-shore and off-shore coastal Alaskan snow, *J. Geophys. Res.*, *117*, D00R12, doi:10.1029/2011JD016639.

Garbarino, J. R., E. Snyder-Conn, T. J. Leiker, and G. L. Hoffman (2002), Contaminants in arctic snow collected over northwest Alaskan sea ice, *Water Air Soil Pollut.*, *139*(1/4), 183–214, doi:10.1023/A:1015808008298.

Goldstein, A. H., and I. E. Galbally (2007), Known and unexplored organic constituents in the Earth's atmosphere, *Environ. Sci. Technol.*, *41*(5), 1514–1521, doi:10.1021/es072476p.

Graber, E. R., and Y. Rudich (2006), Atmospheric HULIS: How humic-like are they? A comprehensive and critical review, *Atmos. Chem. Phys.*, *6*(3), 729–753, doi:10.5194/acp-6-729-2006.

Grannas, A. M., P. B. Shepson, and T. R. Filley (2004), Photochemistry and nature of organic matter in Arctic and Antarctic snow, *Global Biogeochem. Cycles*, *18*, GB1006, doi:10.1029/2003GB002133.

Grannas, A. M., et al. (2007), An overview of snow photochemistry: Evidence, mechanisms and impacts, *Atmos. Chem. Phys.*, *7*(16), 4329–4373, doi:10.5194/acp-7-4329-2007.

Guimbaud, C., et al. (2002), Snowpack processing of acetaldehyde and acetone in the Arctic atmospheric boundary layer, *Atmos. Environ.*, *36*(15–16), 2743–2752, doi:10.1016/S1352-2310(02)00107-3.

Hagler, G. S. W., M. H. Bergin, E. A. Smith, and J. E. Dibb (2007), A summer time series of particulate carbon in the air and snow at Summit, Greenland, *J. Geophys. Res.*, *112*, D21309, doi:10.1029/2007JD008993.

Havers, N., P. Burba, J. Lambert, and D. Klockow (1998), Spectroscopic characterization of humic-like substances in airborne particulate matter, *J. Atmos. Chem.*, *29*(1), 45–54, doi:10.1023/A:1005875225800.

Hecobian, A., X. Zhang, M. Zheng, N. Frank, E. S. Edgerton, and R. J. Weber (2010), Water-Soluble Organic Aerosol material and the light-absorption characteristics of aqueous extracts measured over the southeastern United States, *Atmos. Chem. Phys.*, *10*(13), 5965–5977, doi:10.5194/acp-10-5965-2010.

Hegg, D. A., S. G. Warren, T. C. Grenfell, S. J. Doherty, and A. D. Clarke (2010), Sources of light-absorbing aerosol in arctic snow and their seasonal variation, *Atmos. Chem. Phys.*, *10*(22), 10,923–10,938, doi:10.5194/acp-10-10923-2010.

Honrath, R. E., M. C. Peterson, S. Guo, J. E. Dibb, P. B. Shepson, and B. Campbell (1999), Evidence of NOx production within or upon ice particles in the Greenland snowpack, *Geophys. Res. Lett.*, *26*(6), 695–698, doi:10.1029/1999GL900077.

Honrath, R. E., S. Guo, M. C. Peterson, M. P. Dziobak, J. E. Dibb, and M. A. Arsenault (2000), Photochemical production of gas phase NO from ice crystal NO_3^-, *J. Geophys. Res.*, *105*(D19), 24,183–24,190, doi:10.1029/2000JD900361.

Houdier, S., S. Perrier, F. Dominé, A. Cabanes, L. Legagneux, A. M. Grannas, C. Guimbaud, P. B. Shepson, H. Boudries, and J. W. Bottenheim (2002), Acetaldehyde and acetone in the Arctic snowpack during the ALERT2000 campaign. Snowpack composition, incorporation processes and atmospheric impact, *Atmos. Environ.*, *36*(15–16), 2609–2618, doi:10.1016/S1352-2310(02)00109-7.

Houdier, S., M. Barret, F. Dominé, T. Charbouillot, L. Deguillaume, and D. Voisin (2011), Sensitive determination of glyoxal, methylglyoxal and hydroxyacetaldehyde in environmental water samples by using Dansylacetamidooxyamine derivatization and liquid chromatography/fluorescence, *Anal. Chim. Acta*, *704*, 162–173, doi:10.1016/j.aca.2011.08.002.

Jaffrezo, J., G. Aymoz, C. Delaval, and J. Cozic (2005), Seasonal variations of the water soluble organic carbon mass fraction of aerosol in two valleys of the French Alps, *Atmos. Chem. Phys.*, *5*(10), 2809–2821, doi:10.5194/acp-5-2809-2005.

Kawamura, K., H. Kasukabe, and L. A. Barrie (1996), Source and reaction pathways of dicarboxylic acids, ketoacids and dicarbonyls in arctic aerosols: One year of observations, *Atmos. Environ.*, *30*(10–11), 1709–1722, doi:16/1352-2310(95)00395-9.

King, M. D., and W. R. Simpson (2001), Extinction of UV radiation in Arctic snow at Alert, Canada (82°N), *J. Geophys. Res.*, *106*(D12), 12,499–12,507, doi:10.1029/2001JD900006.

Klánová, J., P. Klán, J. Nosek, and I. Holoubek (2003), Environmental ice photochemistry: Monochlorophenols, *Environ. Sci. Technol.*, *37*(8), 1568–1574, doi:10.1021/es025875n.

Kos, G., and P. A. Ariya (2006), Determination of a wide range of volatile and semivolatile organic compounds in snow by use of solid-phase micro-extraction (SPME), *Anal. Bioanal. Chem.*, *385*(1), 57–66, doi:10.1007/s00216-006-0333-5.

Krivácsy, Z., G. Kiss, D. Ceburnis, G. Jennings, W. Maenhaut, I. Salma, and D. Shooter (2008), Study of water-soluble atmospheric humic matter in urban and marine environments, *Atmos. Res.*, *87*(1), 1–12, doi:10.1016/j.atmosres.2007.04.005.

Lafrenière, M. J., J. M. Blais, M. J. Sharp, and D. W. Schindler (2006), Organochlorine pesticide and polychlorinated biphenyl concentrations in snow, snowmelt, and runoff at Bow Lake, Alberta, *Environ. Sci. Technol.*, *40*(16), 4909–4915, doi:10.1021/es060237g.

Lavanchy, V. M. H., H. W. Gäggeler, U. Schotterer, M. Schwikowski, and U. Baltensperger (1999), Historical record of carbonaceous particle concentrations from a European high-alpine glacier (Colle Gnifetti, Switzerland), *J. Geophys. Res.*, *104*(D17), 21,227–21,236, doi:10.1029/1999JD900408.

Legrand, M., and M. De Angelis (1995), Origins and variations of light carboxylic acids in polar precipitation, *J. Geophys. Res.*, *100*(D1), 1445–1462, doi:10.1029/94JD02614.

Legrand, M., S. Preunkert, M. Schock, M. Cerqueira, A. Kasper-Giebl, J. Afonso, C. Pio, A. Gelencsér, and I. Dombrowski-Etchevers (2007a), Major 20th century changes of carbonaceous aerosol components (EC, WinOC, DOC, HULIS, carboxylic acids, and cellulose) derived from Alpine ice cores, *J. Geophys. Res.*, *112*, D23S11, doi:10.1029/2006JD008080.

Legrand, M., S. Preunkert, T. Oliveira, C. A. Pio, S. Hammer, A. Gelencsér, A. Kasper-Giebl, and P. Laj (2007b), Origin of C2–C5 dicarboxylic acids in the European atmosphere inferred from year-round aerosol study conducted at a west-east transect, *J. Geophys. Res.*, *112*, D23S07, doi:10.1029/2006JD008019.

Lukács, H., et al. (2007), Seasonal trends and possible sources of brown carbon based on 2-year aerosol measurements at six sites in Europe, *J. Geophys. Res.*, *112*, D23S18, doi:10.1029/2006JD008151.

Marbouty, D. (1980), An experimental study of temperature-gradient metamorphism, *J. Glaciol.*, *26*, 303–312.

Matykiewiczová, N., J. Klánová, and P. Klán (2007), Photochemical degradation of PCBs in snow, *Environ. Sci. Technol.*, *41*(24), 8308–8314, doi:10.1021/es0714686.

Mayol-Bracero, O. L., P. Guyon, B. Graham, G. Roberts, M. Andreae, S. Decesari, S. Fuzzi, and P. Artaxo (2002), Water-soluble organic compounds in biomass burning aerosols over Amazonia: 2. Apportionment of the chemical composition and importance of the polyacidic fraction, *J. Geophys. Res.*, *107*(D20), 8091, doi:10.1029/2001JD000522.

Melnikov, S., J. Carroll, A. Gorshkov, S. Vlasov, and S. Dahle (2003), Snow and ice concentrations of selected persistent pollutants in the Ob-Yenisey River watershed, *Sci. Total Environ.*, *306*(1–3), 27–37, doi:10.1016/S0048-9697(02)00482-5.

Meyer, T., and F. Wania (2011), Modeling the elution of organic chemicals from a melting homogeneous snow pack, *Water Res.*, *45*(12), 3627–3637, doi:10.1016/j.watres.2011.04.011.

Meyer, T., Y. D. Lei, I. Muradi, and F. Wania (2009a), Organic contaminant release from melting snow. 1. Influence of chemical partitioning, *Environ. Sci. Technol.*, *43*(3), 657–662, doi:10.1021/es8020217.

Meyer, T., Y. D. Lei, I. Muradi, and F. Wania (2009b), Organic contaminant release from melting snow. 2. Influence of snow pack and melt characteristics, *Environ. Sci. Technol.*, *43*(3), 663–668, doi:10.1021/es8020233.

Moosmüller, H., R. K. Chakrabarty, K. M. Ehlers, and W. P. Arnott (2011), Absorption Ångström coefficient, brown carbon, and aerosols: Basic concepts, bulk matter, and spherical particles, *Atmos. Chem. Phys.*, *11*(3), 1217–1225, doi:10.5194/acp-11-1217-2011.

Narukawa, M., K. Kawamura, S.-M. Li, and J. W. Bottenheim (2002), Dicarboxylic acids in the Arctic aerosols and snowpacks collected during ALERT 2000, *Atmos. Environ.*, *36*(15–16), 2491–2499, doi:16/S1352-2310(02)00126-7.

Perrier, S., S. Houdier, F. Dominé, A. Cabanes, L. Legagneux, A. L. Sumner, and P. B. Shepson (2002), Formaldehyde in Arctic snow: Incorporation into ice particles and evolution in the snowpack, *Atmos. Environ.*, *36*(15–16), 2695–2705, doi:10.1016/S1352-2310(02)00110-3.

Peuravuori, J., and K. Pihlaja (1997), Molecular size distribution and spectroscopic properties of aquatic humic substances, *Anal. Chim. Acta*, *337*(2), 133–149, doi:10.1016/S0003-2670(96)00412-6.

Pinzer, B. R., and M. Schneebeli (2009), Snow metamorphism under alternating temperature gradients: Morphology and recrystallization in surface snow, *Geophys. Res. Lett.*, *36*, L23503, doi:10.1029/2009GL039618.

Ricard, V., J.-L. Jaffrezo, V. Kerminen, R. E. J. Hillamo, M. Sillanpaa, S. Ruellan, C. Liousse, and H. Cachier (2002), Two years of continuous aerosol measurements in northern Finland, *J. Geophys. Res.*, *107*(D11), 4129, doi:10.1029/2001JD000952.

Sun, H., L. Biedermann, and T. C. Bond (2007), Color of brown carbon: A model for ultraviolet and visible light absorption by organic carbon aerosol, *Geophys. Res. Lett.*, *34*, L17813, doi:10.1029/2007GL029797.

Taillandier, A., F. Domine, W. R. Simpson, M. Sturm, T. A. Douglas, and K. Severin (2006), Evolution of the Snow Area Index of the subarctic snowpack in central Alaska over a whole season: Consequences for the air to snow transfer of pollutants, *Environ. Sci. Technol.*, *40*(24), 7521–7527, doi:10.1021/es060842j.

Usenko, S., K. J. Hageman, D. W. Schmedding, G. R. Wilson, and S. L. Simonich (2005), Trace analysis of semivolatile organic compounds in large volume samples of snow, lake water, and groundwater, *Environ. Sci. Technol.*, *39*(16), 6006–6015, doi:10.1021/es0506511.

Warren, S. G., and W. J. Wiscombe (1980), A model for the spectral albedo of snow. II: Snow containing atmospheric aerosols, *J. Atmos. Sci.*, *37*(12), 2734–2745, doi:10.1175/1520-0469(1980)037<2734:AMFTSA>2.0.CO;2.

Yasunari, T. J., R. D. Koster, K. Lau, T. Aoki, Y. C. Sud, T. Yamazaki, H. Motoyoshi, and Y. Kodama (2011), Influence of dust and black carbon on the snow albedo in the NASA Goddard Earth Observing System version 5 land surface model, *J. Geophys. Res.*, *116*, D02210, doi:10.1029/2010JD014861.